

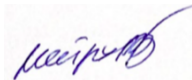



NAZARBAYEV
UNIVERSITY

**Next-generation sequencing for studying microbial
communities during cyanobacterial algal blooms**

Ayagoz Meirkhanova
(B.Sc., Nazarbayev University)

A THESIS SUBMITTED
FOR THE DEGREE OF MASTER OF SCIENCE IN
BIOLOGICAL SCIENCES, DEPARTMENT OF BIOLOGY
SCHOOL OF SCIENCE AND HUMANITIES
NAZARBAYEV UNIVERSITY
2022

Student	Ayagoz Meirkhanova		24/06/2022
Student's Supervisor/Advisor	Natalie Barteneva		24/06/2022

DECLARATION

I hereby declare that the thesis is my original work and it has been written by me in its entirety. I have duly acknowledged all the sources of information which have been used in the thesis. This thesis has also not been submitted for any degree in any university previously.

Ayagoz Meirkhanova

24/06/22

ACKNOWLEDGEMENTS

First and foremost, I would like to express my deepest gratitude to my supervisor Dr. Natalie Barteneva, for her patience, support, and invaluable feedback during my MSc studies. I would like to thank her for providing me with amazing opportunities to explore the field of environmental research and be able to grow as a researcher.

I would also like to extend my sincere thanks to Dr. Thomas Davidson and AU LMWE facility, for a great experience working in Denmark with an incredible team of researchers. Special thanks to Eti Ester Levi, who has helped greatly with metadata necessary for completion of my Master's Thesis.

Many thanks to my lab mates Adina Zhumakhanova and Aidana Baltabekova who shared results of their remarkable analysis on an Imaging Flow Cytometer.

Finally, I would like to thank my family for their unconditional love and support.

TABLE OF CONTENTS

TITLE PAGE	1
DECLARATION	2
ACKNOWLEDGEMENTS	3
TABLE OF CONTENTS	4
ABSTRACT	6
LIST OF TABLES	8
LIST OF FIGURES AND ILLUSTRATIONS	9
ABBREVIATIONS	11
1. INTRODUCTION	12
1.1 Harmful algal blooms (HABs)	12
1.2 Cyanobacterial harmful blooms (CyanoHABs)	12
1.3 Microbial composition during CyanoHABs	14
1.4 Environmental factors affecting CyanoHABs	15
1.4.1 CyanoHABs and climate change	15
1.4.2 CyanoHABs and stratification	15
1.5 Methods to study and monitor CyanoHABs	16
1.5.1 Light microscopy	17
1.5.2 Imaging flow cytometry (IFC)	17
1.5.3 Environmental DNA (eDNA) analysis	17
1.6 Importance	18
2. MATERIALS AND METHODS	18
2.1 Field samples collection	19
2.2 DNA extraction	20
2.3 16S amplicon sequencing	20
2.4 Imaging flow cytometry (IFC) based analysis of microbial community composition	21
2.5 PCR-based functional analysis	21
2.6 Data analysis	22
2.7 Statistical analysis	22
3. AIMS OF THE PROJECT	24
4. RESULTS	25

4.1 Sequencing results	25
4.2 Environmental parameters and mesocosm tanks characteristics	25
4.3 Biodiversity analysis	30
4.3.1 Alpha diversity metrics	30
4.3.2 Beta diversity metrics	34
4.4 Microbial community dynamics	37
4.5 Correlation of results obtained by imaging flow cytometry (IFC) and next-generation sequencing (NGS) methods	40
4.6 Functional analysis (PCR-based)	41
5. DISCUSSION	42
5.1 Effect of environmental parameters on microbial community composition	43
5.2 Effect of stratification on Cyanobacteria	44
5.3 Phytoplankton community dynamics	45
5.4 Correlation of IFC and NGS methods	46
5.5 Limitations	48
6. CONCLUSIONS	48
7. REFERENCE LIST	50
8. APPENDICES	56

Nazarbayev University, School of Sciences and Humanities, Department of Biology
Master's Degree Program of Science in Biological Sciences and Technologies

Ayagoz Meirkhanova: Next-generation sequencing for studying microbial communities during cyanobacterial algal blooms

Master of Science thesis; 65 pages, 12 appendices

Supervisor: Natalie Barteneva, Nazarbayev University, SSH, Department of Biology, natalie.barteneva@nu.edu.kz

Co-supervisor: Christian Schoenbach, Nazarbayev University, SSH, Department of Biology, christian.schoenbach@nu.edu.kz

Keywords: CyanoHAB, next-generation sequencing, 16S rRNA; nanopore-based sequencing; imaging flow cytometry

ABSTRACT

Increasing evidence reports adverse effects of climate change on freshwater ecosystems and harmful algal blooms in particular, but response mechanisms of such heterogeneous communities are poorly understood. Environmental DNA (eDNA) analysis is a suitable and efficient tool for resolving biodiversity within complex ecosystems. Specifically, full-length 16S rRNA next-generation nanopore sequencing, combined with barcoding, was implemented in the work to resolve the structure of plankton communities in LMWE mesocosm experiment. Portable nanopore sequencing technology provides time-efficient and cost-effective analysis of environmental data, with taxonomic resolution up to genera. Since laboratory cultures have limitations in reflecting complex phytoplankton communities, mesocosm facilities were used as experimental setups for studying the variability of these communities. The effect of stratification on microbial composition dynamics was assessed for eight weeks using 12 outdoor mesocosm tanks, with three temperature regimes, varying nutrient levels, and two sampling depths. In total, 192 water samples were collected, followed by eDNA extraction, amplification, and sequencing. Obtained results revealed successful classification (up to 99.93%) of over 1200 genera in each mesocosm tank. Classified taxa of heterotrophic bacteria included low-abundance (<0.01%) genera. Temporal analysis of obtained data revealed changes in microbial dominance throughout the *Microcystis* spp. bloom development. Principal component analysis coupled with ADONIS test revealed a significant correlation between environmental factors and heterotrophic bacteria community composition. Moreover, varying temperature regimes had a significant effect on community structure throughout

the experiment. Microbial communities during stratification and mixing periods were shown to form statistically significant clusters, with *Microcystis* spp. contributing the most to dissimilarity. Obtained results provide insights into the effect of stratification and temperature on microbial community composition.

LIST OF TABLES

Table 1. ADONIS analysis on significance of environmental parameters.

LIST OF FIGURES AND ILLUSTRATIONS

Figure 1. Schematic overview of experimental workflow.

Figure 2. AU LMWE setup of mesocosm tanks. The setup consists of 24 outdoor flow-through mesocosm tanks, which combine 3 varying temperature regimes (ambient temperature, IPCC A2, and IPCC A2+50% climate scenarios), with 2 nutrient levels in 4 replicates.

Figure 3. Environmental parameters throughout the experiment for A tanks. Daily temperature levels (left panel) for surface (lilac), middle (blue) and bottom (green) layers in tanks A1, A2, and A3; daily oxygen levels (right panel) for surface (blue), and bottom (red) layers in tanks A1, A2, and A3. Grey bars indicate periods of stratification (weeks 1, 2, 5 and 6).

Figure 4. Environmental parameters throughout the experiment for D tanks. Daily temperature levels (left panel) for surface (lilac), middle (blue) and bottom (green) layers in tanks D1, D2, and D3; daily oxygen levels (right panel) for surface (blue), and bottom (red) layers in tanks D1, D2, and D3. Grey bars indicate periods of stratification (weeks 1, 2, 5 and 6).

Figure 5. Environmental parameters throughout the experiment for F tanks. Daily temperature levels (left panel) for surface (lilac), middle (blue) and bottom (green) layers in tanks F1, F2, and F3; daily oxygen levels (right panel) for surface (blue), and bottom (red) layers in tanks F1, F2, and F3. Grey bars indicate periods of stratification (weeks 1, 2, 5 and 6).

Figure 6. Environmental parameters throughout the experiment for G tanks. Daily temperature levels (left panel) for surface (lilac), middle (blue) and bottom (green) layers in tanks G1, G2, and G3; daily oxygen levels (right panel) for surface (blue), and bottom (red) layers in tanks G1, G2, and G3. Grey bars indicate periods of stratification (weeks 1, 2, 5 and 6).

Figure 7. Principal component analysis (PCA) of environmental data from mesocosm tanks throughout the experiment. Parameters analyzed include: Temp – temperature, Oxy – oxygen levels, StratInd – stratification index, TP – total phosphorus, pH and PO₄-P levels.

Figure 8. Bar plots of Shannon and Simpson diversity indices for A tanks across three temperature regimes (A1 – ambient, A2 – IPCC A2, A3 – IPCC A2+) and two sampling points (surface and bottom) during stratified and mixed periods.

Figure 9. Bar plots of Shannon and Simpson diversity indices for D tanks across three temperature regimes (D1 – ambient, D2 – IPCC A2, D3 – IPCC A2+) and two sampling points (surface and bottom) during stratified and mixed periods.

Figure 10. Bar plots of Shannon and Simpson diversity indices for F tanks across three temperature regimes (F1 – ambient, F2 – IPCC A2, F3 – IPCC A2+) and two sampling points (surface and bottom) during stratified and mixed periods.

Figure 11. Bar plots of Shannon and Simpson diversity indices for G tanks across three temperature regimes (G1 – ambient, G2 – IPCC A2, G3 – IPCC A2+) and two sampling points (surface and bottom) during stratified and mixed periods.

Figure 12. Multidimensional scaling of Bray–Curtis distance matrix of community compositions throughout the experiment. NMDS ordination plots indicate clustering across varying temperature regimes (AMB - ambient temperature, A2 – IPCC A2, A2+ - IPCC A2+ temperature regime) in tanks A, D, F and G.

Figure 13. Multidimensional scaling of Bray–Curtis distance matrix of community compositions throughout the experiment. NMDS ordination plots indicate clustering across experimental conditions (stratification and mixing periods) in tanks A, D, F and G.

Figure 14. Relative abundance of dominant phyla across 12 tanks at two sampling points (surface and bottom) during the course of the experiment.

Figure 15. Relative abundance of dominant representatives at class level in tanks D1, G1, G2 and G3 at two sampling points (surface and bottom) during the experiment.

Figure 16. Relative abundance of top 10 genera in tank D1 during weeks 1-4 in surface and bottom layers using NGS.

Figure 17. Relative abundance of main phytoplankton classes in tank D1 during weeks 1-4 in surface and bottom layers identified using IFC.

Figure 18. Representation of gel electrophoresis using DNA extracted from G2 tank during the 1st week (stratification) and primers specific for microcystin synthetase gene E (*mcyE*), polysaccharide biosynthesis-related gene cluster (*capD*, *csaB*, *tagH*, *epsL*, *rfbB*, *cpsF*) and genes involved in synthesis of gas vesicles (*gvpC*, *gvpA*).

ABBREVIATIONS

ADONIS	Analysis of variance using distance matrices
HAB	harmful algal bloom
CyanoHAB	cyanobacterial algal bloom
UV	ultraviolet
IFC	imaging flow cytometry
NGS	next-generation sequencing
AU LMWE	Aarhus University Lake Mesocosm Warming Experiment
eDNA	environmental DNA
rRNA	ribosomal RNA
PCR	polymerase chain reaction
NMDS	non-metric multidimensional scaling
PCA	principal component analysis
P	phosphorus
TP	total phosphorus

1. INTRODUCTION

1.1 Harmful algal blooms (HABs)

An alarming increase in the occurrence of “harmful algal blooms” (HABs) has been reported over the last several decades (Anderson et al., 2012). This term refers to the proliferation and accumulation of specific phytoplankton species and covers various types of blooms (Anderson, 2009; Erdner et al., 2008). Phytoplankton represents a polyphyletic group of photosynthetic microorganisms populating euphotic zone in marine, brackish, and freshwater bodies. They form the basis of the aquatic food web and are necessary for supporting the health of aquatic ecosystems (Chisholm, 1992). Accumulation of such organisms can lead to the discoloration of water (most often red, brown, or green tides), formation of surface scums, seafood contamination, and, most importantly, disruption of biogeochemical cycles and food-web dynamics (Anderson, 2009; Friedman and Levin, 2005). HABs can result in depletion of oxygen levels due to high respiration and decomposition rates or, alternatively, can synthesize harmful toxins, which are dangerous to both aquatic organisms and mammals (Sellner et al., 2003). Harmful effects exerted by toxins include but are not limited, to digestive and respiratory problems, seizures, and skin irritation, and affect fish, birds, and humans the most (Sellner et al., 2003). In many parts of the world HABs have already had a great impact on public health, fisheries, and ecosystems, and these impacts are only expected to grow (Gobler, 2020). Despite this fact, the causes behind the increased incidence of blooms are still not clear. Possible explanations range from anthropogenic-related activities, such as water pollution, nutrient enrichment, and climate change, to natural processes of species dispersal (Anderson, 2009; Anderson, 1989; Hallegraeff, 1993; Smayda, 1989). It is thus critical to gain a better understanding of HABs’ development dynamics with future development of mitigation and management strategies.

1.2 Cyanobacterial harmful algal blooms (CyanoHABs)

Cyanobacteria represent a group of oxygenic phototrophic bacteria carrying gram-negative characteristics (Zheng et al., 2013), that can be found in most types of

environments (Whitton and Potts, 2012). Cyanobacterial photosynthetic activity has marked one of the most important evolutionary events on our planet – oxidation of the atmosphere (Schirmer et al., 2015), making them major primary producers (Flombaum et al., 2013; Spungin et al., 2018). Cyanobacteria also produce a wide variety of photosynthetic pigments, such as various forms of chlorophyll, carotenoids, and phycobiliproteins, giving cells a bluish tint responsible for their popular name – “blue-green algae” (Whitton and Potts, 2012). Cyanobacteria carry several unique characteristics allowing them to populate a diverse range of habitats and dominate some of them (Whitton and Potts, 2012). Firstly, most Cyanobacteria reach their maximal growth at higher temperatures compared to most phytoplankton and eukaryotic algae, giving them an advantage in warmer climates (Castenholz and Waterbury, 1989). Cyanobacteria are also adapted to high salinity and desiccation, with some species tolerating high levels of UV radiation (Whitton and Potts, 2012). In addition, most cyanobacterial species contain gas vacuoles – gas-filled vesicles – allowing cyanobacterial cells to control their buoyancy in water columns (Walsby, 1981).

Cyanobacterial species exhibit a wide diversity of forms, with morphology dependent on environmental factors, such as light, temperature, and atmospheric nitrogen fixation (Dick et al., 2021). They carry potentially the greatest impact on aquatic systems due to their ability to produce a wide range of toxic metabolites (cyanotoxins) (Friedman, 2005), with microcystins being one of the well-known ones. Cyanobacterial HABs (cyanoHABs) are of particular interest since cyanobacterial species are one of the most often bloom-forming and have a great impact on both aquatic and terrestrial ecosystems (Hallegraeff, 1993; Komárek and Johansen, 2015). Cyanobacteria are known for their ability to form blooms both in fresh and marine water bodies, with common bloom-forming genera being *Aphanizomenon*, *Nodularia*, *Trichodesmium*, *Planktothrix*, *Dolichospermum*, *Cylindrospermopsis* and *Microcystis* (Huisman et al., 2018).

The incidence of cyanoHABs has increased over the past few decades, as indicated by numerous studies. The trend is only expected to grow with globally increasing rates of eutrophication, CO₂ levels and climate change (Paerl and Huisman, 2008; Paerl and Huisman, 2009; Jöhnk et al., 2008; Wagner and Adrian, 2009; O’Neil et al., 2012; Verspagen et al., 2014). Like other types of algal blooms, cyanoHABs can be detrimental to aquatic ecosystems, causing major water quality issues, depletion of oxygen, and fish

kills (Chorus and Bartram, 1999; Huisman et al., 2005; Paerl and Otten, 2013; Rabalais et al., 2010). As mentioned previously, toxin production is one of the most notable characteristics of cyanobacterial blooms; such toxins have the potential to cause neurological, liver, and digestive damage (Carmichael, 2001; Merel et al., 2013). *Microcystis* spp. blooms are also often associated with the formation of surface scums, which limit the amount of light reaching benthic organisms (Glibert and Burkholder, 2006). In addition, increased respiration rates during such high-biomass blooms lead to depletion of oxygen (hypoxia or anoxia) and subsequent fish kills (Fristachi et al., 2008). Understanding community composition during blooms would therefore, significantly, help in mitigating the potential harmful effects of algal blooms on various aspects of ecosystems and public health.

1.3 Microbial communities composition during CyanoHABs

Complex community dynamics and interactions are one of the most important features of cyanoHABs. Blooms can often affect the composition of microbial communities depending on the stage of the bloom (Huisman et al., 2018). Numerous studies have also pointed out the importance of heterotrophic bacteria in the functioning of cyanobacterial colonies. These bacteria form “cyanospheres” (Alvarenga et al., 2017), and are located in close proximity to cyanobacterial colonies and filaments. Some heterotrophic bacteria have been shown to interact with Cyanobacteria, benefiting from produced fixed nitrogen, organic carbon, and oxygen (Brauer et al., 2015). Such bacteria can either be directly attached to cyanobacterial cells, be part of extracellular polysaccharide sheath, or form free-living populations (Brauer et al., 2015; Ploug et al., 2011; Hmelo et al., 2012). Metagenomic studies on the composition of microbial communities during cyanobacterial blooms revealed that changes in Cyanobacteria-associated bacterial communities reflect changes within cyanobacterial species composition and vice-versa. Moreover, such shifts in community dynamics can also mark different phases of cyanobacterial and algal blooms in general. According to Berg et al. (2018) and Van Hannen et al. (1999), during rapid lysis of cyanobacterial blooms, several representatives of heterotrophic bacteria responsible for the biodegradation of organic molecules become dominant. Similarly, members of class Alphaproteobacteria, which are capable of degradation of microcystin, have been shown to dominate the cyanosphere during the decline of a *Microcystis* bloom.

1.4 Environmental factors affecting CyanoHABs

Several factors influence phytoplankton composition and heterotrophic bacteria during blooms, including temperature, turbulence, light intensity, water acidity, as well as nutrient availability (Cantin et al., 2011; Walsby and Schanz, 2002; Pope and Patel, 2008; Xie et al., 2016; Sanseverino et al., 2022). In addition, the relative importance of Cyanobacteria during blooms can also be determined by these factors. However, response mechanisms of cyanobacterial taxa to environmental factors are not homogenous due to their different ecophysiological properties, therefore requiring better understanding of underlying control processes (Chorus et al., 2021). Evidence suggests that the complex diversity of organisms responsible for the formation of HABs reflects diverse response mechanisms of HABs to environmental changes, which are still yet to be understood. The relationship between HAB dynamics and environmental factors is going to be discussed in the following sections.

CyanoHABs and climate change

Rising temperatures, as a part of climate change, can favor the formation and increased incidence of cyanoHABs in several ways. Firstly, cyanobacterial growth is likely to increase with increasing water temperatures since most cyanobacterial species reach their maximal growth at temperatures above 25°C (Robarts and Zohary, 1987; Paerl and Paul, 2012; Coles and Jones, 2000). Specifically, the optimal temperature for growth and photosynthesis of *Microcystis* spp. were found to be higher or equal to 25.8°C (Paerl and Huisman, 2008; Takamura et al., 1985). Such growth optimum is higher compared to most other phytoplankton and eukaryotic algae, such as dinoflagellates, diatoms, and chlorophytes, favoring the dominance of Cyanobacteria under warmer conditions (Elliott et al., 2006; Jöhnk et al., 2008; Paerl and Huisman, 2009). More importantly, a number of studies indicated an increase in cellular toxin content in several cyanobacterial species with increasing temperatures (Sivonen, 1990; Rapala et al., 1997). As a result, an observed trend in temperature increase can potentially lead to a shift in global phytoplankton community composition in favor of Cyanobacteria.

CyanoHABs and stratification

Apart from the direct effects of rising temperatures on the incidence of cyanoHABs, increased temperatures also lead to warming water surfaces. As a result, water bodies, especially shallow lakes, experience thermal stratification (Paerl and Huisman, 2009; Winder and Sommer, 2012; Wagner and Adrian, 2009; Elliott, 2010). In addition, increased temperatures reduce water densities, further intensifying water column vertical stratification. Longer periods of warmer seasons also suggest an increased period of stratification (Peeters et al., 2007). Consequently, cyanobacterial communities are able to exploit stratified conditions due to their unique feature – control of buoyancy. As mentioned, Cyanobacteria can control their relative position in a water column via gas vesicles. Under turbulent conditions, water mixing distributes cyanobacterial cells preventing them from colony formation. On the contrary, during stratification, buoyant Cyanobacteria float to the water surface, giving them access to optimal light conditions (Walsby, 1981), with further formation of dense scum layer and blooming (Paerl and Huisman, 2009). As a result, increasing evidence suggests that vertical community distribution is just as significant as horizontal, with a complex interplay between the before-mentioned environmental factors and cyanobacterial buoyancy, toxicity, and morphology (Graham and Jones, 2009; Marti et al., 2015; Rowe et al., 2016). In addition, as presented in one of the recent studies conducted by Xiao et al. (2018), colony formation in *Microcystis* has been shown to be affected by turbulence, leading to the formation of different types of colonies. So apart from considering horizontal variation in phytoplankton community composition, which has mostly been the case in previous studies, it is also important to address vertical variation and stratification.

1.5 Methods to study and monitor CyanoHABs

HAB monitoring is an essential task; however, it is particularly complex due to the high degree of both temporal and spatial community composition heterogeneity. In addition, such heterogenous communities' response mechanisms to constantly changing conditions are still poorly understood (Stauffer et al., 2019). Efficient monitoring approach would thus help to (1) understand factors affecting HAB dynamics, (2) detect changes in biomass of species of interest in a timely manner, and (3) indicate the presence of potentially toxic species.

Light microscopy

Classical bloom monitoring typically depends on the morphological identification of species of interest in samples. Species identification has for long been accomplished via light microscopy observation based on already known morphological features for adequate algal characterization (Hallegraeff, 2003). Although traditional light microscopy remains a standard, there are several limitations to the method. It includes the complexity of identifying of certain phytoplankton species, which cannot be easily visualized and/or are unable to discriminate between benign and harmful variants solely based on morphological features. In addition, microscopic analysis is typically time-consuming and requires a high level of experience and expertise. Light microscopy is therefore unsuitable for real-time characterization of heterogenous bloom communities (Sellner et al., 2003).

Imaging flow cytometry (IFC)

Imaging flow cytometry (IFC) is an alternative approach that combines morphological and optical assessment for the detection of phytoplankton. One of such instruments - FlowCAM – is based on fluidic principles used in flow cytometry coupled with light microscopy (Stauffer et al., 2019). It allows the detection of a number different parameters, including size, diameter, etc., and capturing an image of each cell passing through it. Detectable particle size can range from 10 to 1000 μm , which accounts for major algal species (Sellner et al., 2003). In addition, the instrument can operate in a continuous sampling mode with possible portability, holding the potential to monitor algal blooms (Sellner et al., 2003).

Environmental DNA (eDNA) analysis

With advancements in molecular techniques in recent years, their implementation for community studies has become increasingly popular (Esenkulova et al., 2020). Whether in tandem or independently from morphological analysis, molecular studies have successfully applied to resolve community structure in aquatic ecosystems. In particular,

next-generation sequencing, as applied through metabarcoding, has shown its great potential for efficient identification and characterization of phytoplankton assemblages due to its ability to generate massive amounts of sequencing data (Goodwin et al. 2016; Valentini et al. 2016). Specifically, 16S rRNA-based amplicon sequencing is especially efficient in the characterization of community structure during blooms, with possible identification of rare and fragile phytoplankton taxa (Eiler et al. 2011). Genes coding for 16S rRNA subunit can be found in most living organisms, and with the increasing availability of sequence databases, the sequencing approach becomes even more promising.

1.6 Importance

Considering the information discussed above, microbial communities' high spatio-temporal compositional variability during HABs reflects respective changes in environmental factors. In the last decades, climate change and cultural eutrophication have dramatically increased the occurrence of cyanobacterial blooms, and their incidence is only expected to grow. Increasing interest in mitigation of HABs is not only limited to public health safety concerns but also significant economic expenses and losses linked to halted recreational activities, seafood, and drinking water contamination. Given that Cyanobacteria are crucial members of aquatic ecosystems, contributing greatly to the global nutrient cycle, environmental changes, and consequent changes in the frequency of cyanobacterial blooms can potentially inflict long-term changes in aquatic systems.

2. MATERIALS AND METHODS

The experimental part of research was divided into 4 major parts: sample collection, DNA extraction, 16S amplicon sequencing, and downstream analysis. A schematic overview of the workflow is presented in Figure 1.

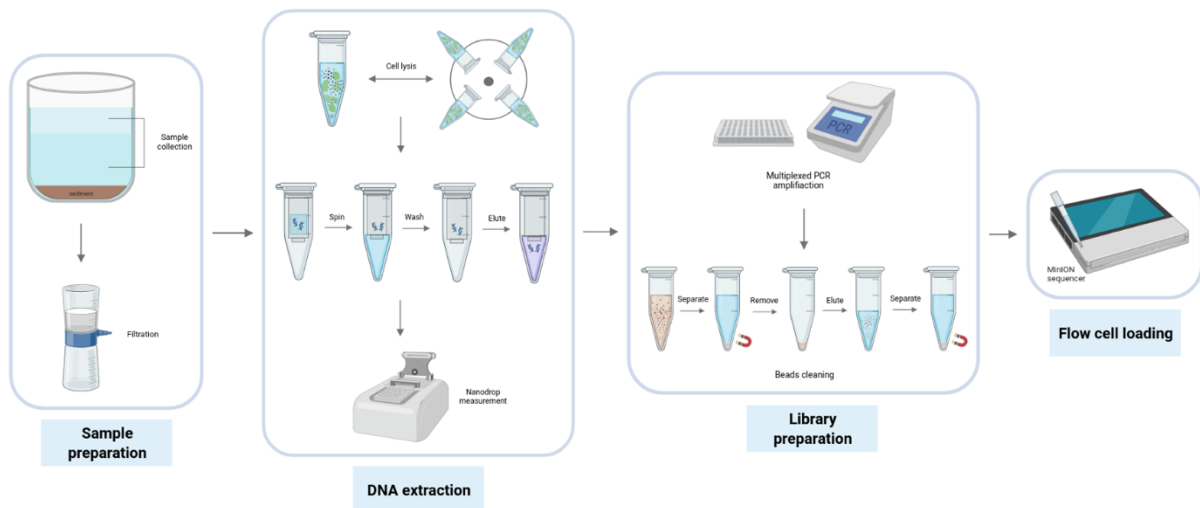


Figure 1. Schematic overview of experimental workflow.

2.1 Field samples collection

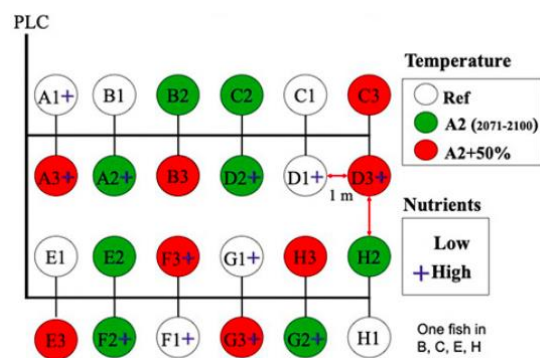


Figure 2. AU LMWE setup of mesocosm tanks. Setup consists of 24 outdoor flow-through mesocosm tanks, which combine 3 varying temperature regimes (ambient temperature, IPCC A2 and IPCC A2+50% climate scenarios) with 2 nutrient levels.

Samples for sequencing analysis were collected at Aarhus University AQUACOSM Lake Mesocosm Warming Experiment (AU LMWE) facility located in Silkeborg, Denmark. It consists of 24 flow-through outdoor mesocosm systems, which represent cylindrical stainless-steel tanks, about 1.9m in diameter and 1.5m in depth. 24 mesocosms combine 3 varying temperature regimes (ambient temperature, IPCC A2 and IPCC A2+50% climate scenarios) with 2 nutrient levels (Figure 2). In addition, mesocosm setups are equipped with temperature, oxygen, as well as pH sensors, providing high-frequency measurements (Liboriussen et al., 2005). Previous year, at LMWE 2021, the effect of temporary stratification on various aspects of the ecosystem was addressed by altering the mixing patterns of mesocosms. To achieve stratification, mixing paddles were

turned off during the period of stratification to allow the system to stratify; moreover, heating elements were moved to the center of the tank – further ensuring stratification. In total, 14 days of mixing were followed by 14 days of stratification during the summer period of July-August'21.

Samples were collected on 8 dates (once per week for 8 weeks in total) from 3 high-nutrient tanks and a control tank (tanks A1-3, D1-3, F1-3, G1-3). Sampling dates are outlined in **Table S1**. Each tank had two sampling points – surface and bottom. Samples for NGS were collected in 500-mL bottles, and later filtered through GF/C filters (Whatman, USA). Filtered samples were then stored in sterile 50-mL Falcon tubes (BD, USA) at -80°C. In total 192 samples were collected and prepared.

2.2 DNA extraction

Sample collection was followed by DNA extraction. For this purpose, DNEasy Power Water Kit (QIAGEN, Germany) was used to extract DNA from filters, following procedures provided by the manufacturer (with an additional lysis step with heating). In general, filtered samples were first lysed via vortexing with beads in a lysis buffer. Then, proteins and inhibitors were removed, and total DNA was captured on a spin column. After elution, 100- μ L of DNA was obtained, and DNA concentrations were measured using Nanodrop spectrophotometer (Thermo Fisher Scientific, USA). Resultant products were stored in 1.5-mL Eppendorf tubes at -20°C.

2.3 16S amplicon sequencing

DNA extraction was followed by library preparation, the first step of which involved PCR amplification. 16S Barcoding Kit 1-24 (SQK-16S024) (Oxford Nanopore Technologies, UK) was used for library preparation; it includes 24 unique barcodes and sequencing adapters necessary for multiplexed sequencing. The full-length 16S gene was amplified using universal 16S primer pair: 27F (5'-AGAGTTTGATCCTGGCTCAG-3') and 1492R (5'-TACGGYTACCTTGTTACGACTT-3'). Library preparation was conducted according to the methodology provided by the manufacturer. The reaction mixture consisted of nuclease-free water (5 μ L), input DNA (10 μ L), LongAmp Hot Start Taq 2X Master Mix (25- μ L), and respective 16S barcode primer (10 μ L). Following parameters were set for the reaction in a thermocycler: 95°C for 1 minute, followed by

25 cycles of 95°C for 20 seconds, 55°C for 30 seconds, 65°C for 2 minutes, and finished by 65°C for 5 minutes. PCR products were then cleaned using AMPure XP beads (Beckman Coulter, USA), and all of the barcoded samples were pooled together in a single Eppendorf tube. The final step of library preparation included the addition of sequencing adapters to the mixture of barcoded samples. Following library preparation, the MinION Mk1C device was prepared for the sequencing run. A flow cell priming kit (EXP-FLP002) was used for priming FLO-MIN106D flow cells. A newly prepared barcoded DNA library was mixed with loading beads and was loaded into the flow cell according to the manufacturer's instructions. The sequencing run was set to about 40-46 hours.

2.4 Imaging flow cytometry (IFC) based analysis of microbial community composition

Collected samples were analyzed in parallel with imaging flow cytometry (IFC) using FlowCAM (Yokogawa Fluid Imaging, USA) flow cytometer. 50 ml water samples were fixed with 1% glutaraldehyde solution and recorded with 10x objective an autoimage mode. Recorded samples were than manually classified using VisualSpreadSheet (version 4.15.1) software and visualized using Prism GraphPad (USA) software.

2.5 PCR-based functional analysis

Based on IFC and NGS analysis, tank G2 was chosen for molecular analysis. Primers used in the study are targeted for the identification of microcystin synthetase gene E (*mcyE*), polysaccharide biosynthesis-related gene cluster (*capD*, *csaB*, *tagH*, *epsL*, *rfbB*, *cpsF*) and genes involved in the synthesis of gas vesicles (*gvpC*, *gvpA*) according to Gan et al. (2012), Chen et al. (2019) and are listed in **Table S2**. The reaction mixture for endpoint PCR consisted of 3 µl of the extracted DNA sample, 25 µl of DreamTaq Hot Start PCR Master Mix, 0.5 µl of each primer (10 µM), and dH₂O up to a final reaction volume of 50 µl. After the preparation of the PCR reaction mixture, samples were transferred to thermocycler (Bio-Rad, USA) and set to 3-min of initial denaturation step at 95°C, followed by 1 cycle of 30s at 95°C, 30s at a temperature depending on melting temperature of each primer and 60s at 72°C. The final extension step included one cycle

of 5min at 72°C. Resultant PCR products were analyzed using gel electrophoresis, namely 1% agarose gel with SYBR Safe DNA Gel Stain (Life Sciences, USA).

2.6 Data analysis

Raw signal data was stored in FAST5 files and underwent basecalling using Guppy neural network-based basecaller integrated into the MinION Mk1C device. Obtained FASTQ files were then processed using Python commands, starting with assessing obtained reads and their quality using the NanoPlot package (<https://github.com/wdecoster/NanoPlot>). This step was followed by quality filtering with a minimum quality score set to 7 (Nanofilt - <https://github.com/wdecoster/nanofilt>), followed by removal of adapter sequences and demultiplexing of reads into respective barcodes (qcat - <https://github.com/nanoporetech/qcat>). Demultiplexed reads were then classified using Kraken2 classification system (<https://github.com/DerrickWood/kraken2>) against the SILVA database, and relative abundances were obtained using Bracken (<https://github.com/jenniferlu717/Bracken>). Vegan R-package and Pavian tool (<https://github.com/fbreitwieser/pavian>) were used for further diversity and taxonomical analyses, as well as the visualization of obtained results.

2.7 Statistical analysis

Diversity indices were used to characterize microbial communities within and between samples. Specifically, alpha diversity metrics, which include Simpson and Shannon indices, were calculated at genus level, and visualized using R package – vegan (version 2.5-7) and PRIMER-7 software in order to analyze communities with respect to their richness and evenness. In addition, beta diversity metrics (Bray-Curtis dissimilarity) were assessed to quantify dissimilarity between communities and were further subjected to non-metric multidimensional scaling (NMDS) using R package – vegan (version 2.5-7) and PRIMER-7 software. Multivariate analysis of variance using distance matrices was applied through “adonis” function (using R package – vegan) to estimate the significance of observed dissimilarities. Moreover, SIMPER analysis was conducted using PRIMER-7 software to calculate the contribution of each species to observed dissimilarity. Principal component analysis (PCA) was used to describe the relationship between community

composition and spatial and environmental variables (pH, temperature, oxygen level, stratification index, TP, and PO₄-P).

3. AIMS OF THE PROJECT

- I. To apply nanopore-based next-generation sequencing for characterization of microbial communities within mesocosm tanks.

- II. To study how microbial communities change in response to an increase in temperature.

- III. To resolve an effect of stratification and mixing periods on microbial communities' dynamics in mesocosm experiment.

4. RESULTS

4.1 Sequencing results

In total, 192 samples across 8 time points have been collected for NGS analysis. Samples were amplified using primer pairs for the full-length 16S gene. Each sampling week was sequenced in a batch of 24 barcodes corresponding to each sampling point for higher throughput. Overall, sequencing runs for 8 time-points yielded a total of 5 559 659, 5 302 319, 6 829 112, 5 372 895, 6 412 082, 3 942 752, 3 445 993, and 3 372 685 reads of high quality ($q>7$), respectively. The number of reads detected in each barcode ranged from 12 070 to 1 139 506 reads; detailed information regarding each sequencing run is present in **Table S3**. Following quality filtering of reads and adapter trimming remaining reads were classified using Kraken2 classification system, which is based on exact k-mer matches for high accuracy and fast classification speeds. SILVA database, which is a comprehensive database of small and large subunit ribosomal RNA sequences, was used as the reference database. Resultant classification rates ranged from 87.93% to 99.93%, and reads were classified down to the genus level. Using taxonomy labels assigned by Kraken 2, the Bracken method was used to compute abundances of species in DNA sequences from barcoded samples detecting up to 1673 genera. Genera with less than 100 reads were excluded from the analysis.

4.2 Environmental parameters and mesocosm tanks characteristics

As outlined in the experimental design, two main stages of plankton community dynamics were achieved over the course of the bloom: stratification and mixing periods. Samples were taken at two depths – surface and bottom – during the whole duration of the experiment. Bottom samples were taken first to minimize the disturbance of stratified layers within water columns. During the experiment, temperature, pH, and oxygen (along with additional parameters) levels have been recorded and varied dramatically across the mesocosm tanks. Oxygen and temperature levels for tanks A (A1, A2, A3) are shown in Figure 3 and range from 15 to 32°C and 1 to 18 mg/L, respectively. As expected, the highest temperatures were achieved in tanks A2 and A3, where elevated temperature regimes were set. Over the period of the experiment, a decline in temperature was observed, which reflects dropping temperatures in Denmark over summer. In general,

oxygen levels in surface layers were more significant than in bottom layers. Trends for temperature and oxygen levels in tanks D (D1, D2, D3), F (F1, F2, F3), and G (G1, G2, G3) are outlined in Figures 4, 5, and 6, respectively. Uneven levels of temperature stratification were achieved across mesocosm tanks. The highest temperature stratification was observed in tanks A1, D1, D2, and D3. Other mesocosm tanks experiencing milder stratification levels. Oxygen stratification was also observed to be uneven across tanks, with tanks A1, A3, D1, D2, D3, F1, and F3 exhibiting higher stratification levels. During mixing periods, tanks generally experienced similar oxygen and temperature levels in surface and bottom layers.

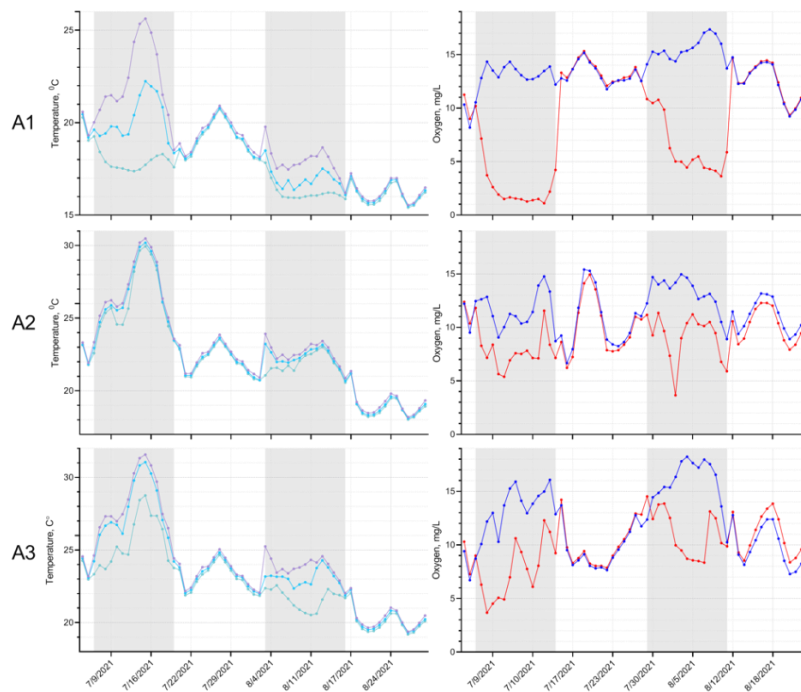


Figure 3. Environmental parameters throughout the experiment for A tanks. Daily temperature levels (left panel) for surface (lilac), middle (blue), and bottom (green) layers in tanks A1, A2, and A3; daily oxygen levels (right panel) for surface (blue) and bottom (red) layers in tanks A1, A2 and A3. Grey bars indicate periods of stratification (weeks 1, 2, 5 and 6).

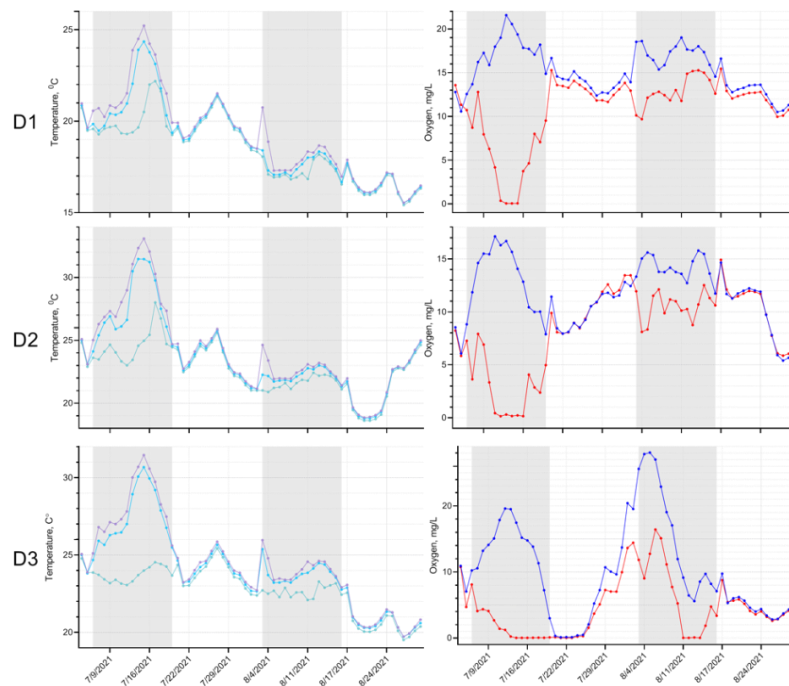


Figure 4. Environmental parameters throughout the experiment for D tanks. Daily temperature levels (left panel) for surface (lilac), middle (blue), and bottom (green) layers in tanks D1, D2, and D3; daily oxygen levels (right panel) for surface (blue) and bottom (red) layers in tanks D1, D2 and D3. Grey bars indicate periods of stratification (weeks 1, 2, 5 and 6).

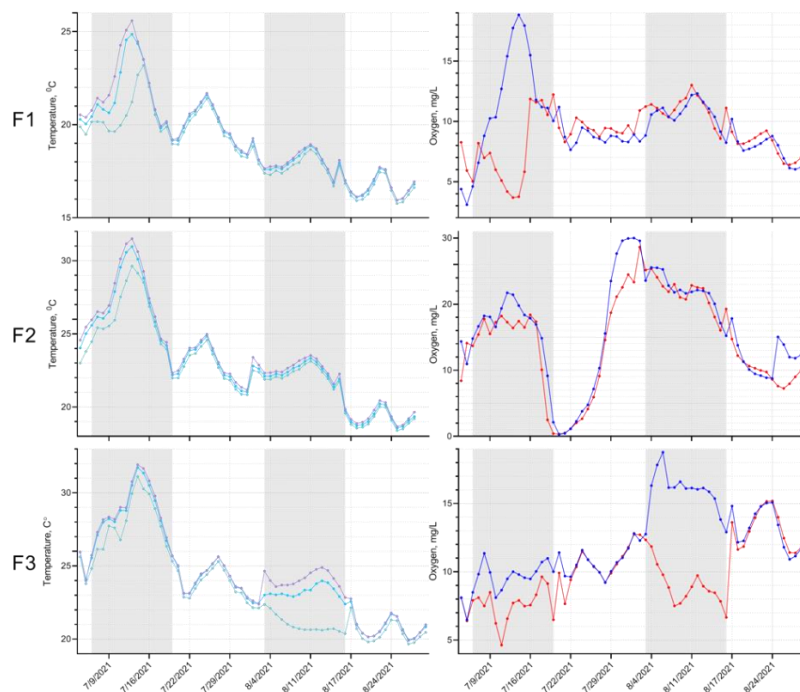


Figure 5. Environmental parameters throughout the experiment for F tanks. Daily temperature levels (left panel) for surface (lilac), middle (blue) and bottom (green) layers in tanks F1, F2 and F3; daily oxygen levels (right panel) for surface (blue), and bottom (red) layers in tanks F1, F2 and F3. Grey bars indicate periods of stratification (weeks 1, 2, 5 and 6).

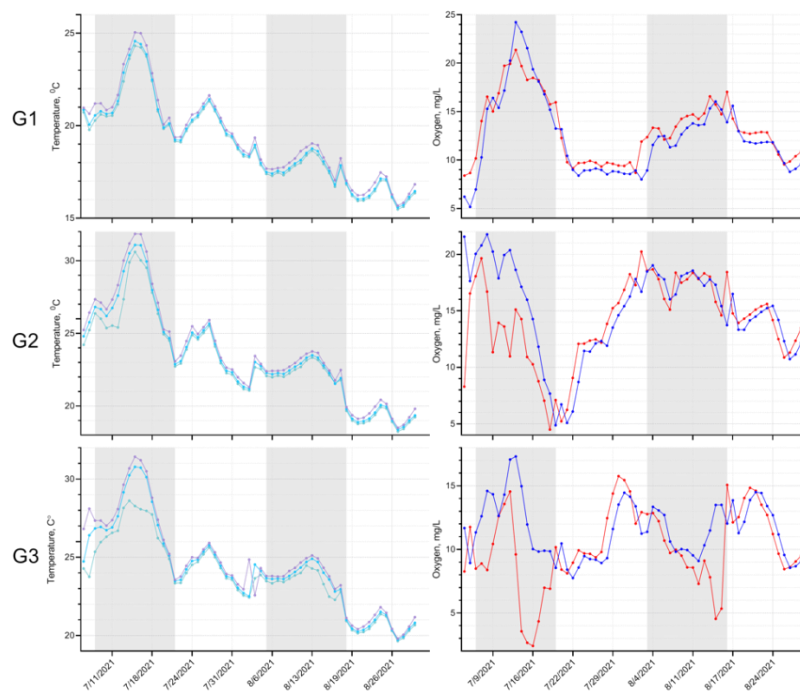


Figure 6. Environmental parameters throughout the experiment for G tanks. Daily temperature levels (left panel) for surface (lilac), middle (blue), and bottom (green) layers in tanks G1, G2, and G3; daily oxygen levels (right panel) for surface (blue) and bottom (red) layers in tanks G1, G2 and G3. Grey bars indicate periods of stratification (weeks 1, 2, 5 and 6).

PCA analysis was conducted using distance matrices to determine a set of environmental parameters that best described community structure within tanks (Figure 7). Temperature, oxygen, pH, total phosphorus (TP), $\text{PO}_4\text{-P}$ levels, and stratification index were analyzed. Analysis of variance using distance matrices (ADONIS) coupled with permutation test with pseudo- F ratios revealed that almost all parameters were significant in describing community structure (**Table 1**). pH and $\text{PO}_4\text{-P}$ levels were not significant in tanks A during the experiment. In addition, the stratification index was shown to have no significant effect on community composition in tanks F and G, which is supported by temperature and oxygen levels in those tanks.

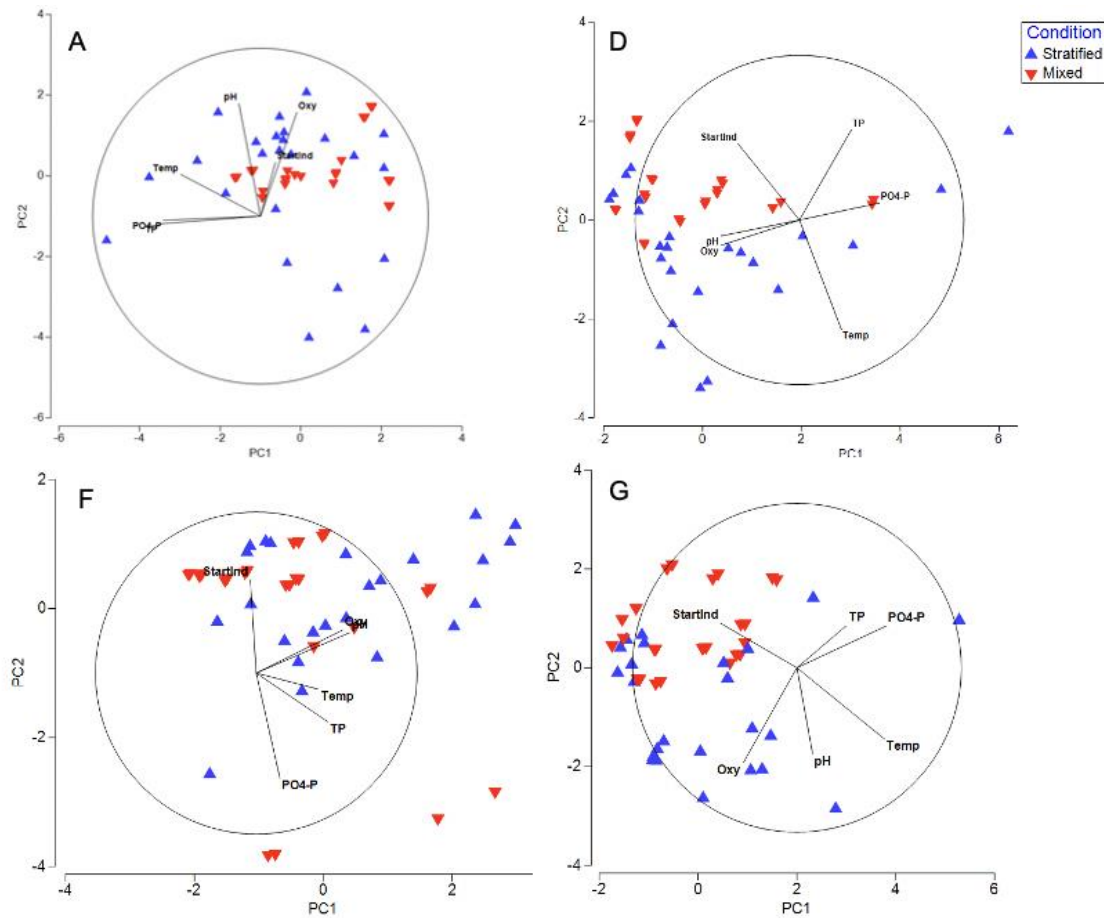


Figure 7. Principal component analysis (PCA) of environmental data from mesocosm tanks throughout the experiment. Parameters analyzed include: Temp – temperature, Oxy – oxygen levels, StratInd – stratification index, TP – total phosphorus, pH and PO₄-P levels.

Table 1. Multivariate analysis of variance using distance matrices on significance of environmental parameters.

Parameter	A	D	F	G
<i>Temperature</i>	0.001 (***)	0.001 (***)	0.006 (**)	0.005 (**)
<i>Oxygen</i>	0.044 (*)	0.005 (**)	0.001 (***)	0.001 (***)
<i>pH</i>	0.14	0.004 (**)	0.002 (**)	0.013 (*)
<i>Stratification index</i>	0.002 (**)	0.008 (**)	0.127	0.428
<i>TP</i>	0.032 (*)	0.019 (*)	0.001 (***)	0.001 (***)
<i>PO₄-P</i>	0.063	0.035 (*)	0.003 (**)	0.001 (***)

4.3 Biodiversity analysis

Alpha diversity metrics

To evaluate changes in biodiversity within mesocosm tanks across eight time points, variations in Shannon and Simpson indices (relative abundance of genera) for microbial communities were calculated and are presented in Figures 8-11. Both Shannon and Simpson indices indicate that communities during stratified periods (week 1, 2, 5, 6) were generally higher in diversity compared to mixed periods (week 3, 4, 7, 8) in tank A1. With increasing temperature conditions (IPCC A2 and IPCC A2+ regimes), surface layers in tanks A during both stratified and mixed periods have higher diversity indices. Differences between community richness between surface and bottom layers were better observed in tanks D (Figure 9). While the ambient temperature regime indicates similar diversity indices in both surface and bottom layers, at higher temperatures (tanks D2 and D3), surface layers appear to have greater species diversity. Similar observations can be made for tanks F (Figure 10). Lastly, only tank G3 has appeared to have greater genera diversity in surface layers during stratified periods (Figure 11).

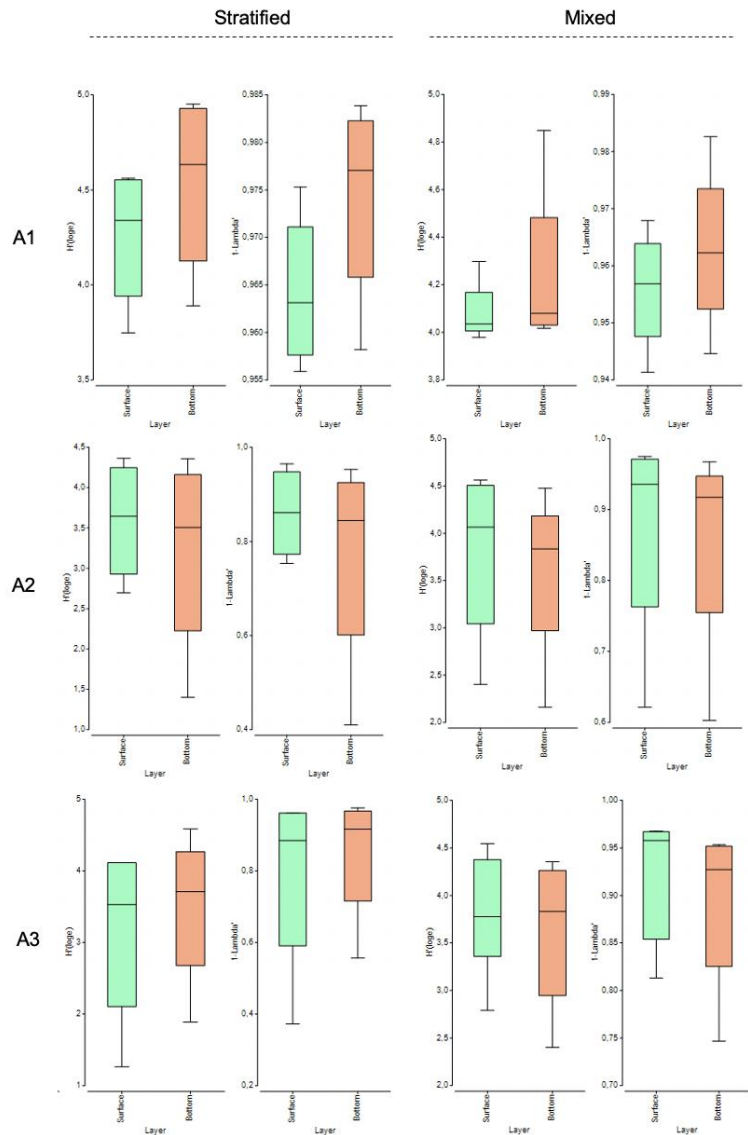


Figure 8. Bar plots of Shannon and Simpson diversity indices for A tanks across three temperature regimes (A1 – ambient, A2 – IPCC A2, A3 – IPCC A2+) and two sampling points (surface and bottom) during stratified and mixed periods.

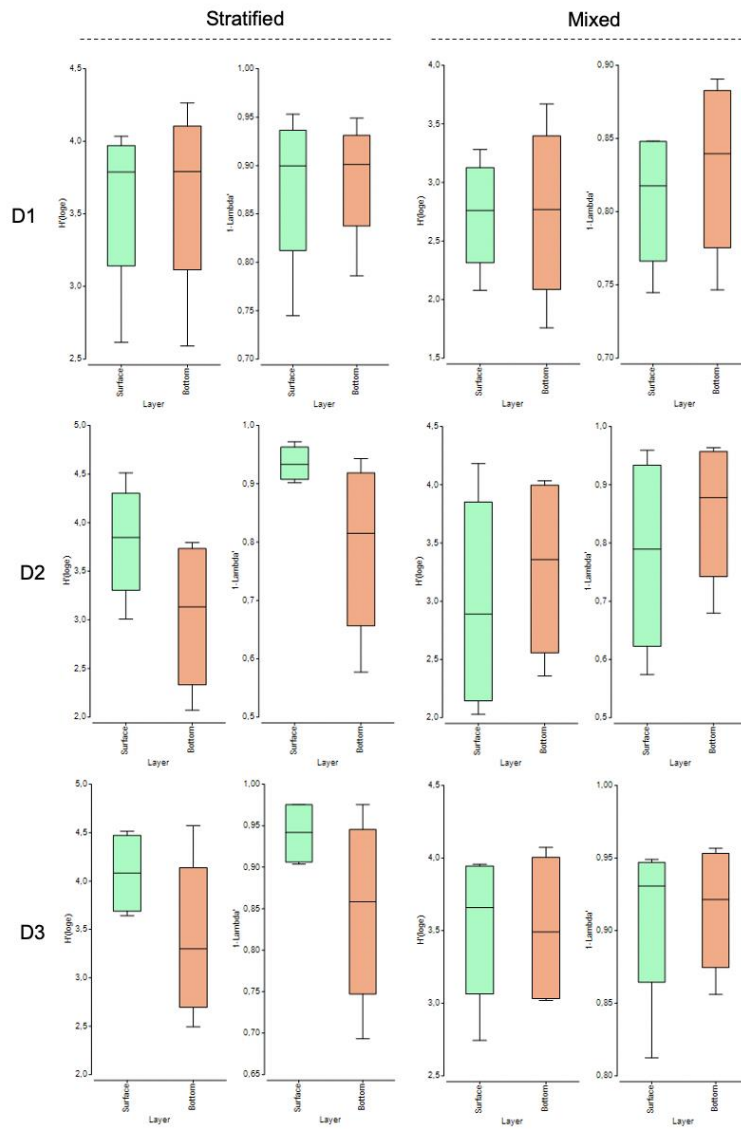


Figure 9. Bar plots of Shannon and Simpson diversity indices for D tanks across three temperature regimes (D1 – ambient, D2 – IPCC A2, D3 – IPCC A2+) and two sampling points (surface and bottom) during stratified and mixed periods.

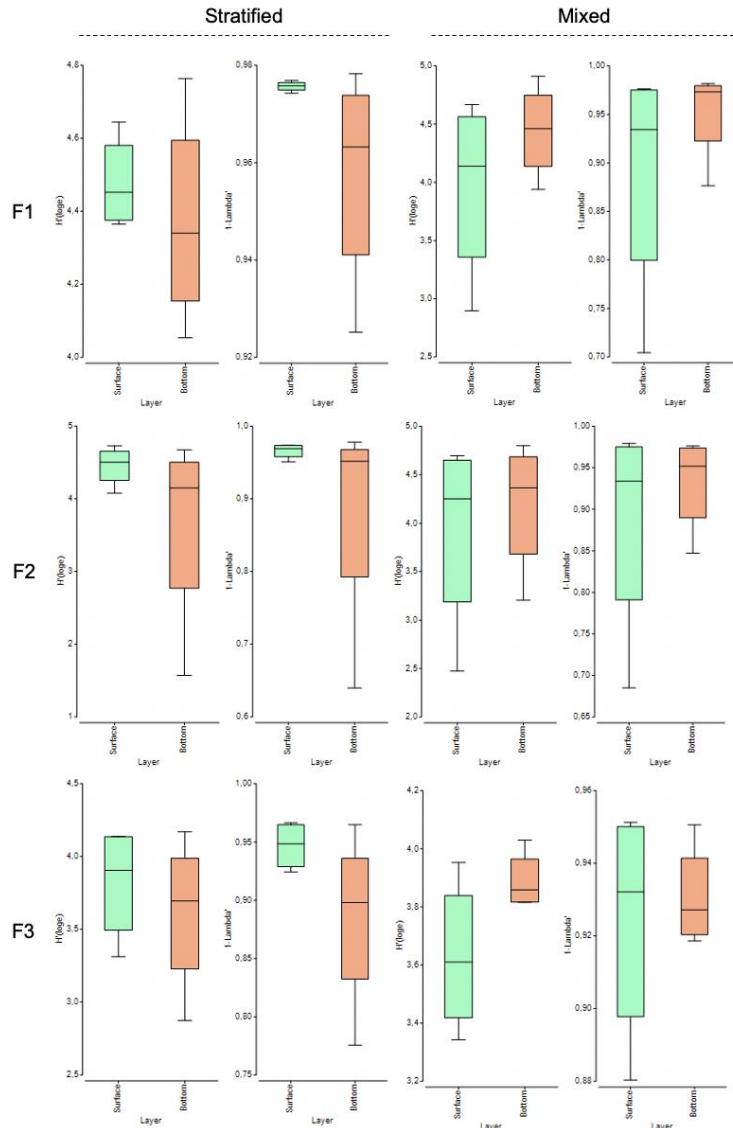


Figure 10. Bar plots of Shannon and Simpson diversity indices for F tanks across three temperature regimes (F1 – ambient, F2 – IPCC A2, F3 – IPCC A2+) and two sampling points (surface and bottom) during stratified and mixed periods.

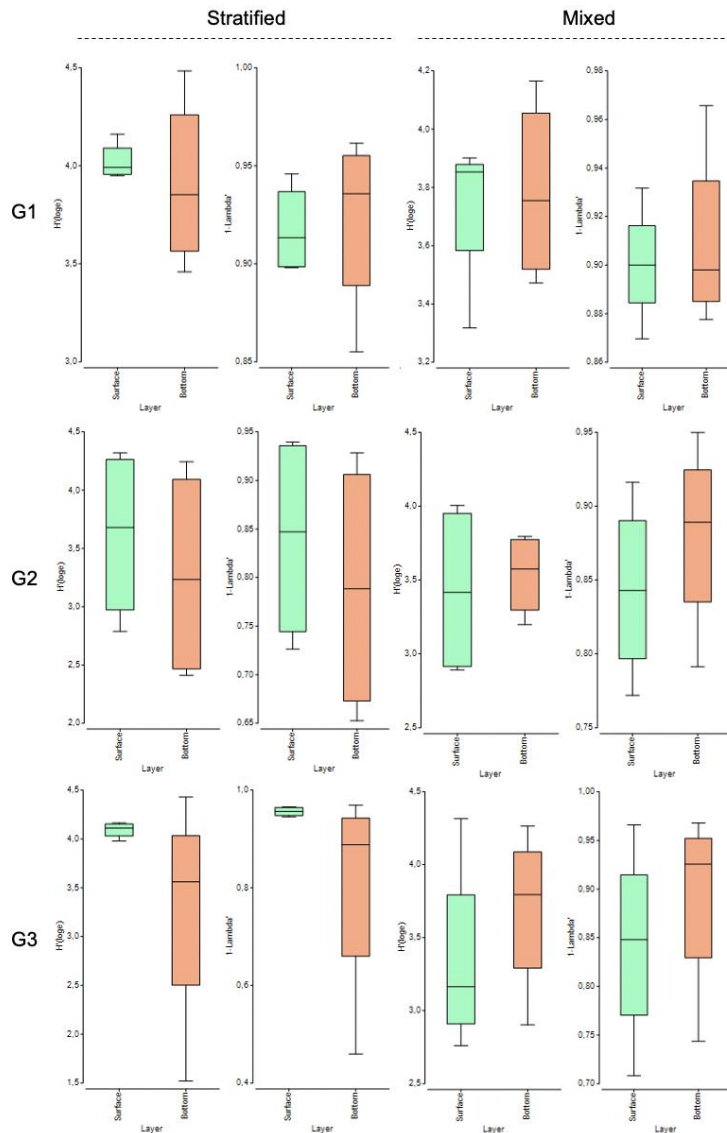


Figure 11. Bar plots of Shannon and Simpson diversity indices for G tanks across three temperature regimes (G1 – ambient, G2 – IPCC A2, G3 – IPCC A2+) and two sampling points (surface and bottom) during stratified and mixed periods.

Beta diversity metrics

Temperature patterns in microbial community biodiversity as measured through the Bray-Curtis dissimilarity matrix in nMDS space are shown in Figure 12. According to it, clustering of tanks based on varying temperature regimes was observed throughout the experiment. Specifically, pairwise ADONIS analysis revealed a significant difference between phytoplankton communities in tanks A with AMB and IPCC A2 regimes ($R=0.407$, $p<0.001$); between AMB and IPCC A2+ ($R=0.219$, $p<0.001$); and between IPCC A2 and IPCC A2+ ($R=0.165$, $p<0.003$). In addition, SIMPER analysis indicates that the average Bray-Curtis similarity between all pairs of sites in A tanks with AMB

regime is 67.82%, with top contributors being *Pseudomonas* (2.04% out of 3.01%), *Comamonas* (1.38% out of 2.03%) and *Limnohabitans* (1.38% out of 2.03%) genera. The average similarity in IPCC A2 regime communities is 63.69%, with top contributors being *Pseudomonas* (3.64% out of 5.74%), *Escherichia-Shigella* (1.10% out of 1.73%), and *Flavobacterium* (0.89% out of 1.40%) genera. Lastly, the average similarity in IPCC A2+ regime communities is 57.26%, with top contributors being *Pseudomonas* (3.04% out of 7.06%), *Escherichia-Shigella* (1.37% out of 2.39%), and *Acidovorax* (1.23% out of 2.16%).

A similar analysis was conducted for the rest of the tanks. Pairwise ADONIS analysis has also revealed a significant difference between phytoplankton communities in tanks D with AMB and IPCC A2 regimes ($R=0.455$, $p<0.001$); between AMB and IPCC A2+ ($R=0.632$, $p<0.001$); and between IPCC A2 and IPCC A2+ ($R=0.171$, $p<0.003$). Unlike communities in tank A, the average similarity (55.2%) of communities in tanks D with AMB regime was contributed most by *Microcystis PCC-7914* (5.36% out of 9.7%), followed by *Pseudomonas* (4.52% out of 8.19%) and *Coleofasciculus PCC-7420* (1.46% out of 1.96%). The average similarity in IPCC A2 regime communities is 57.71%, with top contributors being *Pseudomonas* (3.78% out of 7.31%), *Escherichia-Shigella* (1.35% out of 2.61%), and *Flavobacterium* (1.45% out of 2.8%) genera. Lastly, the average similarity in IPCC A2+ regime communities is 54.65%, with top contributors being *Pseudomonas* (2.43% out of 4.45%), *Escherichia-Shigella* (1.30% out of 2.38%), and *Flavobacterium* (1.12% out of 2.06%).

Significant differences between temperature regimes in tanks F were observed as well (AMB-IPCC A2: $R=0.5$, $p<0.001$; AMB-IPCC A2+: $R=0.481$, $p<0.001$; IPCC A2-IPCC A2+: $R=0.532$, $p<0.001$). Similar to tanks A, similarities within communities with AMB and IPCC A2 regimes were contributed most by *Pseudomonas*, *Escherichia-Shigella*, along with *Massilia* genera. Communities with IPCC A2+ regime were mostly contributed by *Pseudomonas*, *Limnohabitans*, and *Comamonas* genera.

Lastly, significant differences between temperature regimes in tanks G were also observed (AMB-IPCC A2: $R=0.268$, $p<0.001$; AMB-IPCC A2+: $R=0.641$, $p<0.001$; IPCC A2-IPCC A2+: $R=0.523$, $p<0.001$). Similar to tanks D, similarities within communities with regimes AMB and IPCC A2 were most contributed by *Microcystis PCC-7914*, *Pseudomonas* and *Escherichia-Shigella* genera. Communities with IPCC

A2+ regime were mostly contributed by *Pseudomonas*, *Flavobacterium*, and *Limnohabitans* genera.

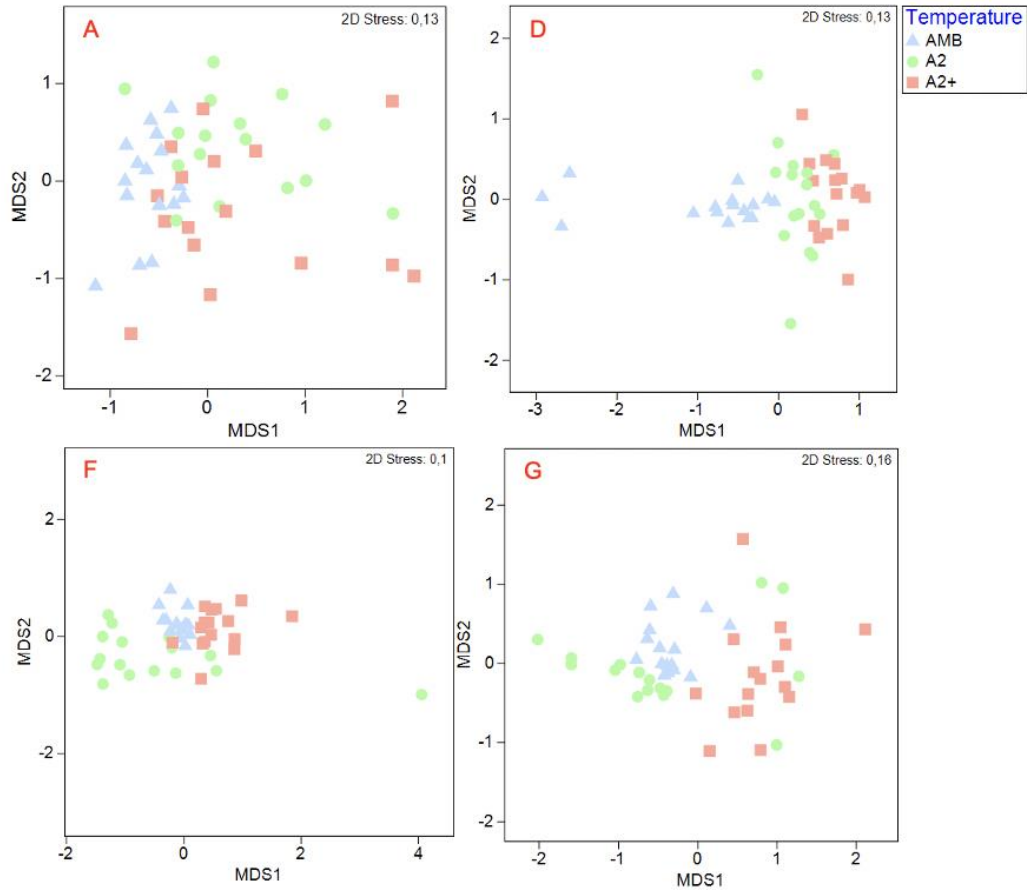


Figure 12. Multidimensional scaling of Bray–Curtis distance matrix of community compositions throughout the experiment. NMDS ordination plots indicate clustering across varying temperature regimes (AMB - ambient temperature, A2 – IPCC A2, A2+ - IPCC A2+ temperature regime) in tanks A, D, F, and G.

In addition to nMDS clustering based on temperature, significant differences between communities during stratification and mixing periods were observed (Figure 13). ADONIS analysis revealed a significant difference between phytoplankton communities in tanks A during stratified and mixed conditions ($R=0.043$, $p<0.044$), with *Pseudomonas* genera contributing the most to the observed dissimilarity between two clusters (0.96% out of 2.38%). Tanks D have also formed significantly distinct clusters ($R=0.069$, $p<0.019$), with *Microcystis* PCC-7420 contributing the most to dissimilarity (1.2% out of 2.2%). Lastly, ANOSIM analysis also revealed significant differences between clusters in tanks F ($R=0.06$, $p<0.024$), with *Pseudomonas* contributing the most to dissimilarity

(0.76% out of 1.84%). No significant differences were observed in tanks G. In addition to nMDS analysis, observed dissimilarities across tanks between surface and bottom layers are graphically illustrated in Supplementary Figures S2-S9 using Bray-Curtis distance matrices and estimated bootstrap averages in nMDS space.

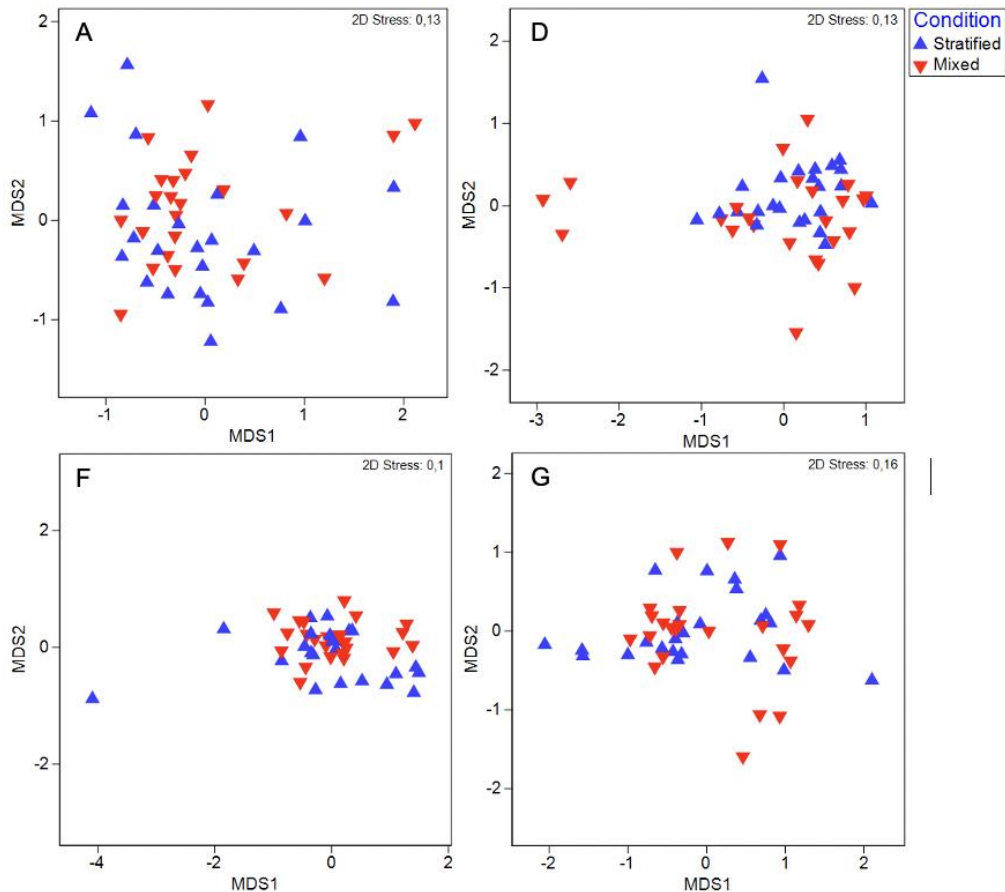


Figure 13. Multidimensional scaling of Bray–Curtis distance matrix of community compositions throughout the experiment. NMDS ordination plots indicate clustering across experimental conditions (stratification and mixing periods) in tanks A, D, F, and G.

4.4 Microbial community dynamics

Microbial community composition and dynamics at the phylum level during the experiment are shown in Figure 14. Proteobacteria, Bacteroidetes, Firmicutes, as well as Cyanobacteria were the major dominant phyla in most tanks, along with all 8 time points. Taxonomic analysis revealed that Proteobacteria phylum dominated nearly all tanks during these weeks, with relative abundance reaching its maximum at 97.89% in tank A2 during the 2nd week. Gammaproteobacteria and Alphaproteobacteria were the dominant class within Proteobacteria phylum during the beginning of the stratification period (week

1), followed by Cyanobacteria and Bacteroidia. This trend was observed throughout the first 4 weeks; however, tank G2 was an exception, where the dominance of Cyanobacteria phylum was observed, both at the surface and bottom layers. Tank G2 during weeks 1 and 2, which both correspond to stratified conditions, was dominated by Cyanobacteria phylum (74.86 and 67.55%, respectively), but a sharp decline in its abundance is seen during weeks 3 and 4 – about 36.6% (mixed conditions). Tanks D1 and G1 appear to be additional tanks, other than G2, to host cyanobacterial species the most. In addition, mixing weeks (3, 4, 7, 8) appear to be denser in terms of phyla composition in comparison to stratified weeks.

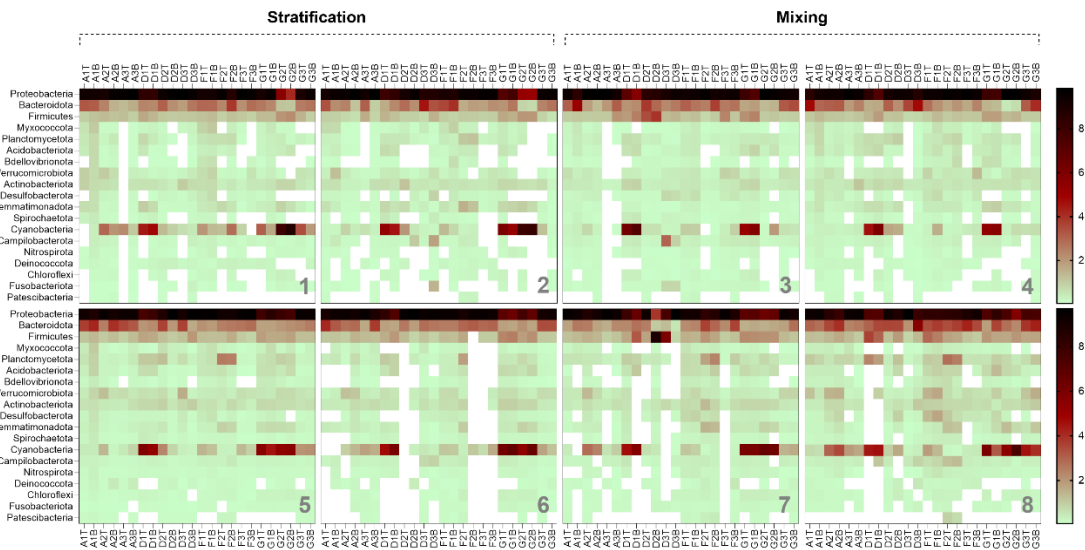


Figure 14. Relative abundance of dominant phyla across 12 tanks at two sampling points (surface and bottom) during the course of the experiment.

Interesting community dynamics were observed at the class level in tanks D1, G1, G2, and G3, where cyanobacterial genera were present the most (Figure 15). Gammaproteobacteria mostly dominate both top and bottom layers of tank D1 during all 8 weeks of the experiment. However, Cyanobacteria take over the dominance at the beginning of mixing week (week 3) but proceed to drop further in relative abundance. A similar pattern is observed in the tank G1, where at the end of the 2nd stratification period (week 6), cyanobacterial representatives outnumber Gammaproteobacteria but drop in their abundance with the increasing number of Gammaproteobacterial genera. In tank G2, a stronger correlation between the abundance of Gammaproteobacteria and Cyanobacteria can be seen. During the beginning of the 1st mixing period (week 3) sharp

decline of cyanobacterial abundance is corresponded to a sharp incline of Gammaproteobacteria. Tank G3 was mainly dominated by Gammaproteobacteria, with little presence of Cyanobacteria.

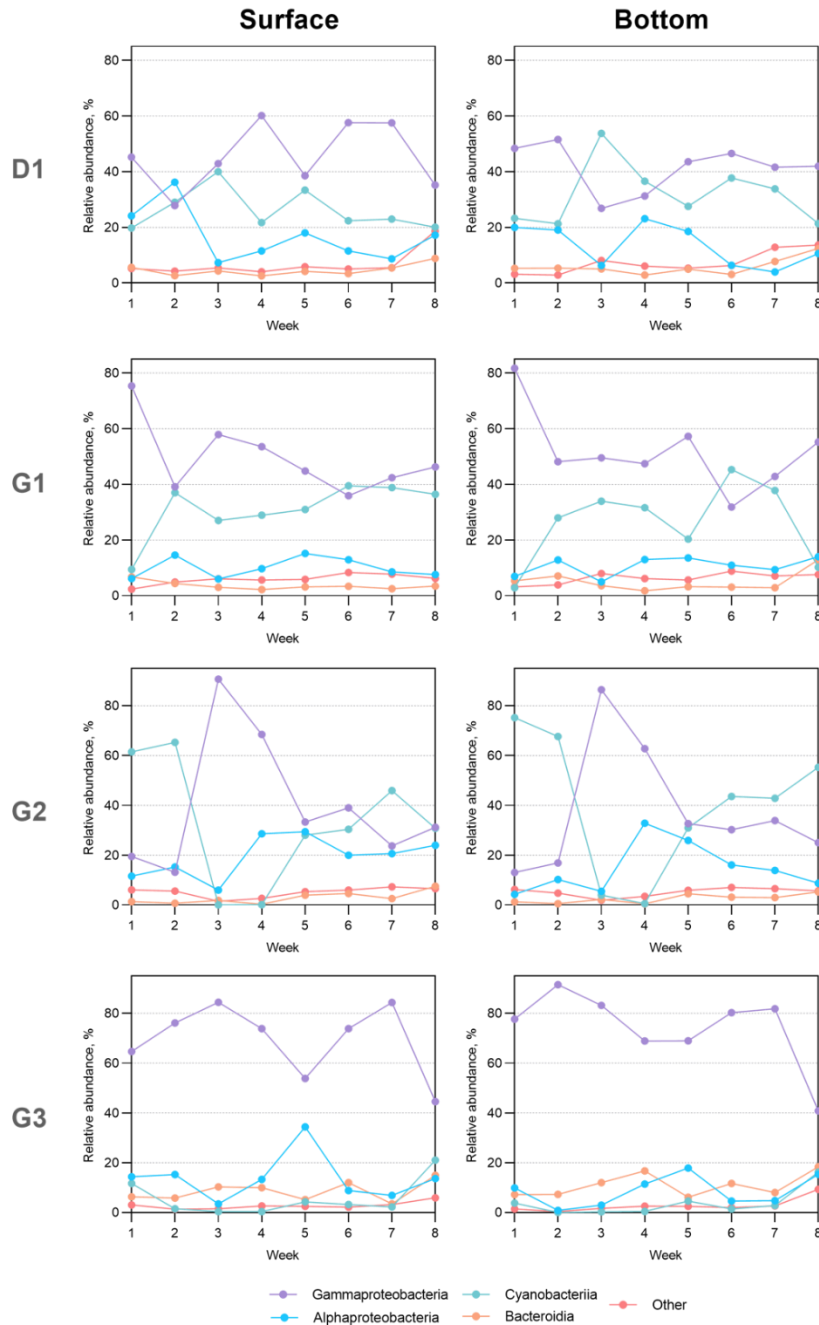


Figure 15. Relative abundance of dominant representatives at class level in tanks D1, G1, G2 and G3 at two sampling points (surface and bottom) during the experiment.

4.5 Correlation of results obtained by imaging flow cytometry (IFC) and next-generation sequencing (NGS) methods

Phytoplankton communities were analyzed by NGS in parallel with Imaging Flow Cytometry (IFC), and classification results of NGS and IFC were compared. According to taxonomical classification results obtained using NGS for tank D1 during the first 4 weeks of the experiment (Figure 16), varying dominance of heterotrophic bacteria can be observed. During the beginning of stratification (week 1), tank D1 was dominated by representatives of the *Microcystis* genus in the top and bottom layers. However, a succession of dominance from *Microcystis* to *Pseudomonas* during 2nd week of stratification in the bottom layer can be observed. Week 3 (mixing) reveals an interesting trend, with *Pseudomonas* genera increasing in its relative abundance and with *Microcystis* becoming dominant in the bottom layer. At the end of mixing (week 4), surface layers are dominated by *Pseudomonas*, while a large proportion of the community in the bottom layer is dominated by *Microcystis*.

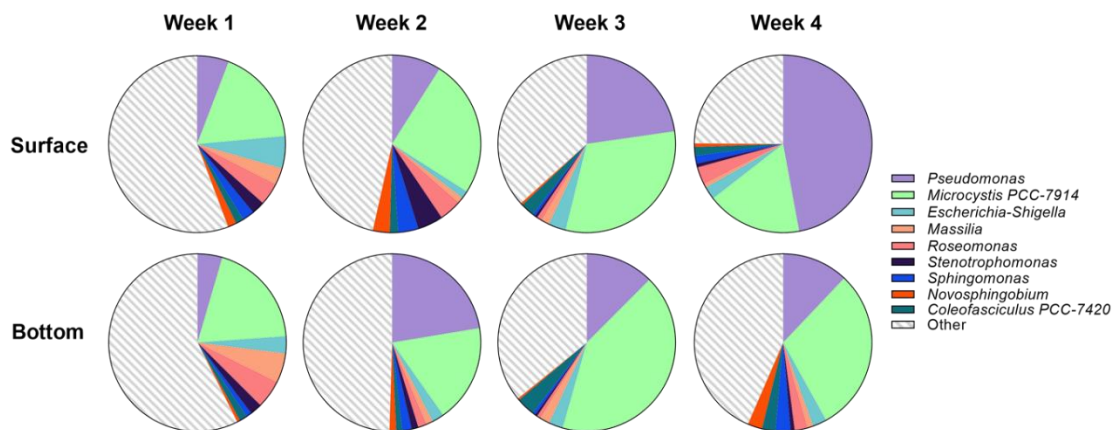


Figure 16. Relative abundance of top 10 genera in tank D1 during weeks 1-4 in surface and bottom layers using NGS.

Results obtained using IFC reveal slightly different community composition dynamics in tank D1 (Figure 17). Similar to NGS analysis, the microbial community during the 1st week was dominated by both colonial and unicellular *Microcystis*. However, with progressing stratification (week 2) and subsequent mixing period (week 3), a decline in the relative abundance of *Microcystis* in the top layer of tank D1 was observed, with the bottom layer remaining relatively the same. The end of the mixing period (week 4) was characterized by a slightly declined abundance of *Microcystis* in the bottom layer,

consistent with NGS analysis. Apart from *Microcystis*, bigger members of the phytoplankton community, such as *Cryptomonas*, *Scenedesmus*, *Pediastrum*, and diatoms, were detected during weeks 3 and 4.

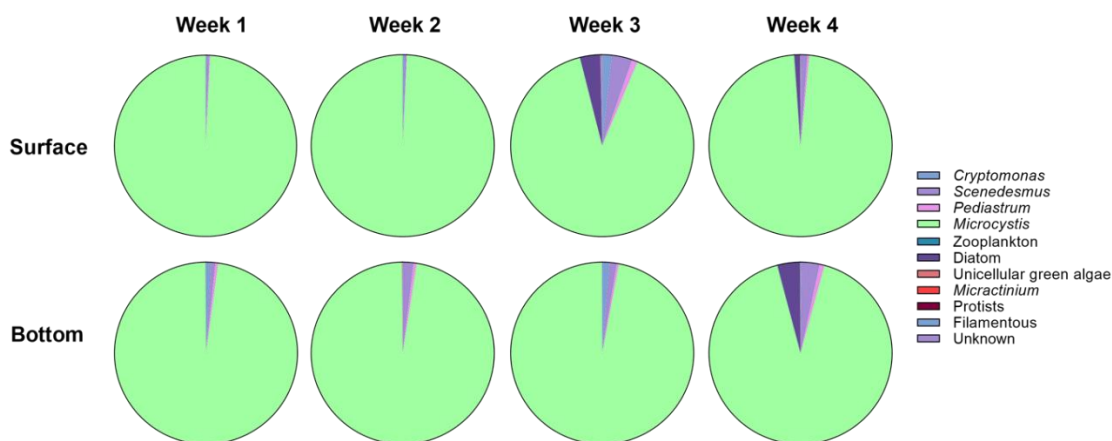


Figure 17. Relative abundance of main phytoplankton classes in tank D1 during weeks 1-4 in surface and bottom layers identified using IFC.

4.6 Functional analysis (PCR-based)

Based on the detection of functional genes mentioned previously, the functional potential of microbial communities could be deduced. Tank G2 was chosen as a sample for the detection of genes responsible for toxin synthesis (*mcyE*), polysaccharide biosynthesis-related gene cluster (*capD*, *csaB*, *tagH*, *epsL*, *rfbB*, *cpsF*) and genes involved in the synthesis of gas vesicles (*gvpC*, *gvpA*) via PCR method, due to the highest relative abundance of *Microcystis* representatives. Primers used in this step were successfully synthesized according to Gan and colleagues (2012) and Chen and co-authors (2018) and are outlined in **Table S2**. PCR reaction was conducted according to the outlined procedure with annealing temperatures for primers *capD*, *tagH*, *rfbB* and *gvpC* set for 65.5°C; *csaB*, *epsL*, *cpsF* and *gvpA* with annealing temperature 62.5°C; *mcyE* – 51.6°C. Agarose gel electrophoresis of obtained PCR products revealed distinct bands corresponding to *mcyE*, *capD*, *csaB* and *tagH* genes (Figure 18). A faint band near 250bp (referenced by 1Kb ladder) was also observed for *rfbB*. NCBI nucleotide BLAST tool was used in order to calculate the size of expected PCR products. *Microcystis aeruginosa* NIES-843 whole-genome sequence was used as a reference, and the expected

product sizes for each gene were calculated as follows: *mcyE* – 246bp, *capD* – 275bp, *csaB* – 287bp, *tagH* – 242bp, *rfbB* – 148bp, which correlate with band sizes obtained using gel electrophoresis. PCR products of genes involved in gas vesicle synthesis were not detected with above-mentioned set of primers.

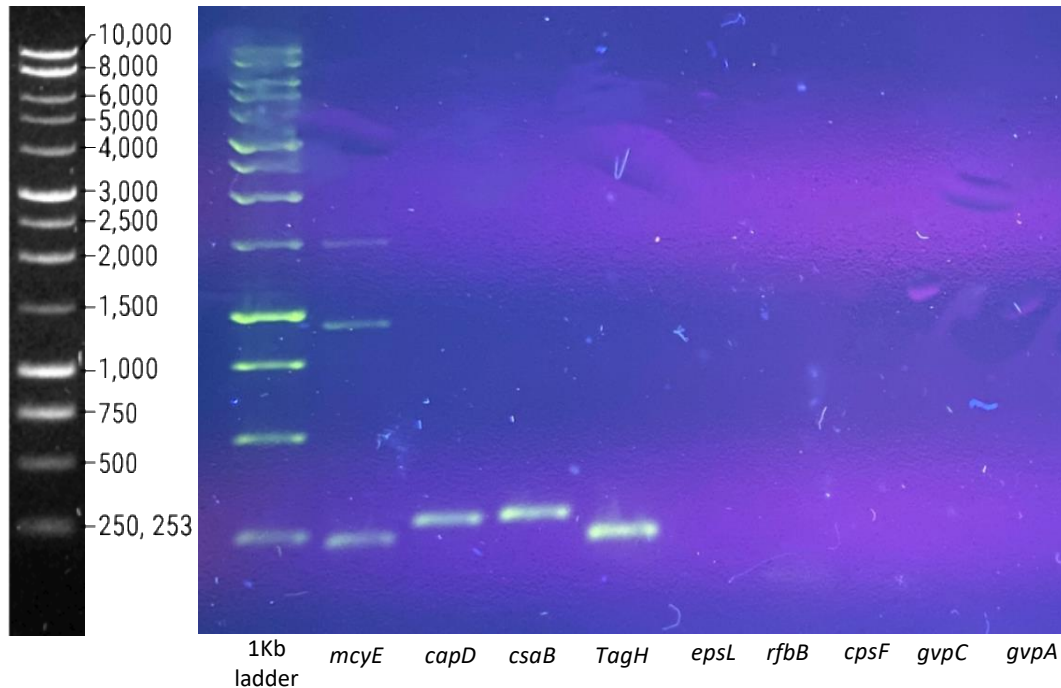


Figure 18. Representation of gel electrophoresis using DNA extracted from G2 tank during the 1st week (stratification) and primers specific for microcystin synthetase gene E (*mcyE*), polysaccharide biosynthesis-related gene cluster (*capD*, *csaB*, *tagH*, *epsL*, *rfbB*, *cpsF*) and genes involved in synthesis of gas vesicles (*gvpC*, *gvpA*).

5. DISCUSSION

An increasing number of research points out the importance of microbial interactions within aquatic ecosystems due to their potential to impact global nutrient cycling, biogeochemical cycles, and community biodiversity (Kouzuma and Watanabe, 2015). However, this area remains open to debate, as not much is understood regarding mechanisms regulating the dynamics of these complex interactions. Published literature has addressed the effects of chemical and physical parameters on cyanobacterial bloom composition, with limited information on the overall Cyanobacteria-associated microbial community (Berg et al., 2008). In this work, we investigated spatial and temporal composition of microbial communities under simulated stratification conditions in

mesocosm facilities. Specifically, NGS methods, applied through metabarcoding, allowed us to investigate and provide insights into underlying microbial interactions and mechanisms regulating these processes. Successful application of nanopore-based sequencing of 192 water samples from 12 different mesocosm tanks with varying temperature regimes, nutrient levels, and mixing conditions is reported. 16S rRNA-based amplicon sequencing was the method of choice, as it provides for comprehensive taxonomic profiles of microbiota within mesocosm tanks.

5.1 Effect of environmental parameters on microbial community composition

Abiotic (environmental parameters, such as nutrient availability and hydrochemical parameters) and biotic (such as aquatic plants and grazers) factors have for long been regarded as the main drivers of biodiversity within phytoplankton communities (Worden et al., 2015). CyanoHABs, in particular, have been shown to be affected by multiple biotic and abiotic factors, with the temperature being one of the major ones. Under normal conditions – during cold summers – *Microcystis* can float up to the surface, forming moderate blooms. However, due to the unfavorable growth temperature, such blooms remain limited in terms of their size and toxicity. It is not the case when elevated temperatures (such as during hot summers) are present. Under such conditions, *Microcystis* can reach its maximum growth rates due to the higher temperature growth optimum of Cyanobacteria compared to other phytoplankton groups – about 25°C (Jöhnk et al., 2008; Paerl, 2009; Coles and Jones, 2000). As a result, increased temperatures allow Cyanobacteria to outcompete other primary producers, mainly dinoflagellates, diatoms, cryptophytes, and chlorophytes (Jöhnk et al., 2008; Elliott et al., 2006).

Among the environmental parameters analyzed in this work, the temperature strongly correlates with community biodiversity within all mesocosm tanks. These results are consistent with previous studies and indicate that temperature is one of the major factors affecting microbial community composition during mixing and stratification periods (Niu et al., 2011; Hampton et al., 2014). As a result, short-term microbial succession was observed in mesocosm tanks, with a temperature being one of the main drivers of microbial community composition. This trend was especially apparent in tanks D and G, where the highest in comparison to other mesocosm tanks nutrient load can be observed. In addition to temperature, other environmental parameters were analyzed, including pH,

oxygen, TP, and PO₄-P levels. Similar to temperature, these factors were also found to be significant in determining phytoplankton composition within mesocosm tanks. Tanks A were an exception, as pH was revealed to have no significant effect on community structure. In addition, the stratification index was also found to be statistically insignificant in shaping communities in tanks F and G, indicating that these tanks possibly did not stratify completely during the experiment.

5.2 Effect of stratification on Cyanobacteria

Apart from the direct effect of elevated temperatures on growth rates of cyanobacterial species, an increase in temperature also promotes an increase in surface water temperature, thereby leading to strong water bodies' stratification while also suppressing its vertical mixing (Jöhnk et al., 2008). Reduced vertical turbulence similar to elevated temperature allows Cyanobacteria, like *Microcystis*, to outcompete other phytoplankton groups. Cyanobacteria can synthesize gas vesicles, allowing them to control their buoyancy, which provides buoyant species with a competitive advantage for light over non-buoyant phytoplankton (Huisman et al., 2004). Several studies confirmed the development of surface blooms by buoyant Cyanobacteria during heatwaves (Fernald et al., 2007; Jöhnk et al., 2008). Higher temperatures can also lead to reduced water viscosity, further promoting floatation of buoyant cyanobacterial species to surface waters (Jöhnk et al., 2008; Paerl and Huisman, 2009). With little wind mixing, water columns stratify even further, allowing Cyanobacteria to float to the surface of the waterbody. Such accumulation of cyanobacterial cells, given high temperatures, leads to dense cyanobacterial blooms. Therefore, the competitive advantage of Cyanobacteria allows them to sustain their photosynthetic needs at high irradiance (Paerl et al., 1983; Huisman et al., 2004). Long-term survival under such high-irradiance conditions is ensured by the presence of photoprotective accessory pigments, such as scytonemins and carotenoids, possessed by several taxa (Paerl and Huisman, 2009). As mentioned previously, most bloom-forming Cyanobacteria can control their relative position in a water column by carefully balancing their buoyancy using cellular gas vesicles while simultaneously accumulating carbohydrates as a form of ballast (Kromkamp and Walsby, 1990; Visser et al., 1995). Therefore, increased rates of stratification coupled with decreased water viscosity favor rapid adjustment of Cyanobacteria within water column, allowing for

optimization of their nutrient and light needs. In addition, Cyanobacteria shade non-buoyant phytoplankton beneath, further outcompeting other phytoplankton (Huisman et al., 2004; Jöhnk et al., 2008).

According to the results presented by Elliott et al. (2006), increased temperatures exert different effects on oligotrophic and eutrophic waters. In other words, in oligotrophic water bodies, which are characterized as low-nutrient systems, the development of high-density cyanobacterial blooms is prevented by limited nutrient levels. As mentioned earlier, warming water surfaces increase vertical stratification in water columns, thus limiting upward flux of nutrients (Sarmiento et al., 2004). As a result, reduced nutrient flux can lead to reduced phytoplankton growth (Schmittner, 2005; Huisman et al., 2006). On the other hand, in eutrophic waterbodies, which are rich in nutrients, nutrient levels are not limited to growth factors (Joehnk et al., 2008). In such case, light availability becomes a critical factor in determining phytoplankton composition, by restricting the growth of certain species. Cyanobacteria, being able to control their relative position in a water column using gas vesicles, are thus able to outcompete non-buoyant phytoplankton (Walsby et al., 1997; Huisman et al., 2004). As a result, eutrophic waterbodies are especially susceptible to dense cyanobacterial blooms during periods of increased temperatures. Our results support this observation, as *Microcystis* PCC-7420 was found to be a major contributing factor to dissimilarity between stratified and mixed conditions genera in tanks D (high-nutrient mesocosms). However, non-metric multidimensional scaling (nMDS) analysis revealed no significant differences between surface and bottom layers in mesocosm tanks.

5.3 Microbial community dynamics in *Microcystis*-dominated community

As mentioned previously, Cyanobacteria are among the dominant phyla in eutrophic lakes. It is partially achieved by cyanobacterial colony formation leading to larger populations of cyanobacterial cells and dense, toxic, surface blooms. Maintenance of such dense populations not only requires sufficient light and nutrients, but also additional morphological and physiological adaptive mechanisms (Shen et al., 2011). One of such is formation of mucilaginous layer, which has several possible functional implications, one of which is embedment of heterotrophic bacteria (Brunberg, 1999). PCR analysis has revealed presence of several *Microcystis*-specific polysaccharide biosynthesis-related

genes such as *capD*, *csaB* and *tagH*. Previously, *capD* and *tagH* genes were reported to be related to capsular polysaccharide biosynthesis (Gan et al., 2012), and *csaB* was associated with exopolysaccharide (methanolan) synthesis (Cava et al., 2004). As a result, possible interaction mechanisms between cyanobacterial cells and surrounding microbial community within mucilaginous layer can range from nutrient cycling to growth inhibition (Ozaki et al., 2008). Under natural conditions *Microcystis* occurs mainly as a colonial form, however, axenic laboratory cultures have shown *Microcystis* to be grown as unicellular entities (Shen et al., 2011). This in turn suggests that surrounding microbial communities may possibly play a role in shaping cyanobacterial colonies, with interactions being generally mutualistic (Berg et al., 2008). A number of co-culturing experiments have revealed specific interactions between *Microcystis* and associated bacteria, such as direct or indirect lysis of *Microcystis* cells, degradation of microcystin (Lemes et al., 2008) and exchange of nutrients. As a result, *Microcystis* could potentially provide an environment suitable for the growth of heterotrophic bacteria, which in turn contributes to nutrient cycling in such systems (Brunberg, 1999; Shen et al., 2011). In this work, dynamics of several phytoplankton classes in relation to Cyanobacteria were analyzed; they include Gammaproteobacteria, Alphaproteobacteria and Bacteroidia. Mesocosm tanks were mostly dominated by Gammaproteobacterial representatives, however, relative abundance of Cyanobacteria was found to be inversely correlated to the abundance of Gammaproteobacteria. Earlier stages of algal blooms are rich in carbohydrates and organic acids, which in turn can serve as chemoattractants for Gammaproteobacterial groups (Buchan et al., 2014). In addition, abundance of Alphaproteobacteria throughout the experiment was found to be correlated to the abundance of Cyanobacteria to some degree. Alphaproteobacterial family Sphingomonadaceae was previously reported to degrade microcystins, and thus usually persists during the later stages of the bloom.

5.4 IFC in characterization of *Microcystis* dominated community

To correlate changes in microbial communities with *Microcystis*-dominated cyanobacterial bloom development we use IFC-based approach in parallel with 16S NGS. Harmful algal blooms require efficient monitoring systems for timely response to the effects of these blooms. A number of options are available, among which DNA-based

monitoring techniques have proven to be especially powerful. With high detection capabilities and high-throughput potential, methods like next-generation sequencing allow identification and characterization of members of microbial communities, with the potential to distinguish closely related species, toxic and non-toxic variants of the same species, as well as rare taxa (Feist and Lance, 2021). Conventional methods, such as light microscopy, which rely on visual inspection of samples of interest, are less efficient in community composition analysis of complex algal ecosystems. It requires a high level of experience and expertise and often fails to discriminate toxic and/or rare species (Humbert et al., 2010; Brooks et al., 2017). Optical methods remain standard when it comes to species identification; however, HAB monitoring requires efficient, sensitive, and specific methods for successful mitigation of harmful effects of algal blooms. In addition, HAB monitoring is a challenging task, as analysis of biologically diverse eDNA samples requires accurate identification and characterization of bloom-participating species. Such eDNA samples contain mixes of numerous heterogenous taxa, identification of which can often be complicated.

In this work, nanopore next-generation sequencing was implemented to resolve complex phytoplankton communities in mesocosm tanks. Universal primers were used during the process of DNA metabarcoding to amplify the DNA sequence of interest (16S rRNA) across various taxa. As a result, by targeting regions of DNA conserved across multiple organisms, such as ribosomal RNA, simultaneous detection of various taxa was possible in multiple samples in parallel. NGS-based characterization of the microbial community in tank D1 revealed varying dominance of *Microcystis* genus throughout the first three weeks of the experiment. The majority of dominant genera in tank D1 belonged to Proteobacteria (*Stenotrophomonas*, *Pseudomonas*, *Arenimonas*, *Massilia*, *Escherichia-Shigella*, *Limonohabitans*, *Brevundimonas*, *Acinetobacterium*, *Acidovorax*, *Variovorax*) and Bacteroidota (*Flavobacterium*) phyla. Apart from *Microcystis* PCC-7914, other cyanobacterial strains included *Synechocystis* CCALA 700, *Cylindrospermum* PCC-7417, *Nostoc* PCC-7107 strains. Results have shown that the IFC-based approach successfully identifies the beforementioned eukaryotic phytoplankton, as well as zooplankton. Another feature of IFC analysis includes the ability to differentiate between colonial and non-colonial morphoforms of *Microcystis*, which is not resolved on the 16S rRNA level due to high levels of genetic similarity. As

a result, an integrative approach of both optical and molecular methods is needed for a comprehensive assessment of microbial communities. While NGS is essential for identifying of prokaryotic and picoplanktonic communities, IFC is needed for the characterization of larger eukaryotic groups, as well as *Microcystis* morphospecies. In addition, DNA-based methods can potentially be the best-suited approach for long-term monitoring of HAB community composition, dynamics of which are significantly influenced by continuously changing environmental factors and biotic interactions. A wider application of NGS-based taxonomic identification in the analysis of freshwater communities would provide more insights into HAB formation dynamics with possible prediction modeling. Metagenomics is particularly useful for the identification of potential biological controls of cyanoHABs.

5.5 Limitations

Presented work carries several potential limitations. Firstly, 16S rRNA-based taxonomic profiling of phytoplankton communities is limited to existing databases, which need to be regularly updated. It can often be complicated because most microbial species are not cultivable under laboratory conditions, and their isolation for sequencing can be challenging. As a result, such members of phytoplankton communities may not be detected using 16S rRNA-based amplicon sequencing. In addition, 16S rRNA-based taxonomic profiling is limited to the identification of prokaryotes and prokaryotic phytoplankton, failing to recognize eukaryotic phytoplankton, such as diatoms, dinoflagellates, cryptomonads, and others. Therefore, results obtained solely based on the 16S rRNA gene could potentially be misinterpreted. Regarding the experimental setup, mesocosm tanks are limited in terms of their size. AU LMWE mesocosm is 1.5 meters deep, while shallow lakes are usually 3 to 4.5 meters deep. It could explain that no significant difference between phytoplankton communities in surface and bottom layers was observed. Moreover, the length of stratification periods could potentially be prolonged in order to ensure better stratification of layers within mesocosm tanks.

6. CONCLUSIONS

In this work, the successful application of nanopore-based sequencing technology for studying the spatial and temporal composition of microbial communities during

cyanobacterial bloom was demonstrated. Specifically, 16s rRNA-based amplicon sequencing was used to reveal the effect of stratification on microbial communities within mesocosm tanks with varying temperature regimes and nutrient levels. Varying stratification levels were achieved in mesocosm tanks, resulting in different responses of microbial communities in all tanks. PCA analysis, however, revealed a significant correlation between environmental parameters, such as pH, oxygen, TP and PO₄-P levels, and microbial community structure. In addition, strong clustering of microbial communities within tanks based on temperature regimes was observed. The temperature was therefore found to be one of the leading factors driving diversity within microbial communities.

Importantly, phytoplankton assemblages during stratification periods were found to be significantly different from those during mixed periods; *Microcystis* PCC-7420 was found to be the dominant strain contributing to the before-mentioned dissimilarity in tanks with a high nutrient load. 16s rRNA-based taxonomic profiles of each mesocosm tank revealed highly heterogeneous microbial communities with complex microbial succession dynamics. Moreover, IFC analysis was found to be successful in detecting *Microcystis* spp., along with several members of eukaryotic algae, as well as grazers. Therefore, comprehensive assessment of microbial communities requires an integrative approach of both optical and molecular methods. Obtained results highlight complex microbial interactions during algal blooms; understanding of such interactions is essential for successful mitigation of harmful effects of cyanobacterial algal blooms.

7. REFERENCE LIST

- Alvarenga D, Fiore M & Varani A (2017) A Metagenomic Approach to Cyanobacterial Genomics. *Frontiers in Microbiology* 8:809
- Anderson D (2009) Approaches to monitoring, control and management of harmful algal blooms (HABs). *Ocean & Coastal Management* 52: 342-347
- Anderson D, Cembella A & Hallegraeff G (2012) Progress in Understanding Harmful Algal Blooms: Paradigm Shifts and New Technologies for Research, Monitoring, and Management. *Annual Review of Marine Science* 4: 143-176
- Anderson DM (1989) Toxic algal blooms and red tides: a global perspective. In: *Red tides: biology, environmental science and toxicology* pp. 11-16. Elsevier
- Berg C, Dupont C, Asplund-Samuelsson J, Celepli N, Eiler A, Allen A, Ekman M, Bergman B & Ininbergs K (2018) Dissection of Microbial Community Functions during a Cyanobacterial Bloom in the Baltic Sea via Metatranscriptomics. *Frontiers in Marine Science* 5:55
- Berg K, Lyra C, Sivonen K, Paulin L, Suomalainen S, Tuomi P & Rapala J (2008) High diversity of cultivable heterotrophic bacteria in association with cyanobacterial water blooms. *The ISME Journal* 3: 314-325
- Brauer V, Stomp M, Bouvier T, Fouilland E, Lebourlangier C, Confurius-Guns V, Weissing F, Stal L & Huisman J (2015) Competition and facilitation between the marine nitrogen-fixing cyanobacterium *Cyanothece* and its associated bacterial community. *Frontiers in Microbiology* 5:795
- Brooks B, Lazorchak J, Howard M, Johnson M, Morton S, Perkins D, Reavie E, Scott G, Smith S & Steevens J (2017) In some places, in some cases, and at some times, harmful algal blooms are the greatest threat to inland water quality. *Environmental Toxicology and Chemistry* 36: 1125-1127.
- Brunberg A (1999) Contribution of bacteria in the mucilage of *Microcystis* spp. (Cyanobacteria) to benthic and pelagic bacterial production in a hypereutrophic lake. *FEMS Microbiology Ecology* 29: 13-22
- Buchan A, LeClerc GR, Gulvik CA, González JM (2014) Master recyclers: features and functions of bacteria associated with phytoplankton blooms. *Nature Reviews Microbiology* 12(10), 686-698
- Cantin A, Beisner B, Gunn J, Prairie Y & Winter J (2011) Effects of thermocline deepening on lake plankton communities. *Canadian Journal of Fisheries and Aquatic Sciences* 68: 260-276.
- Carmichael W (2001) Health Effects of Toxin-Producing Cyanobacteria: "The CyanoHABs". *Human and Ecological Risk Assessment: An International Journal* 7: 1393-1407
- Castenholz RW, Waterbury JB (1989) Cyanobacteria. In: *Bergey's manual of systematic bacteriology* pp 1710-1727. Baltimore: Williams & Wilkins
- Cava F, De Pedro M, Schwarz H, Henne A & Berenguer J (2004) Binding to pyruvylated compounds as an ancestral mechanism to anchor the outer envelope in primitive bacteria. *Molecular Microbiology* 52: 677-690

- Chen M, Tian L, Ren C, Xu C, Wang Y & Li L (2019) Extracellular polysaccharide synthesis in a bloom-forming strain of *Microcystis aeruginosa*: implications for colonization and buoyancy. *Scientific Reports* 9:1251
- Chisholm SW (1992) Phytoplankton size. In: *Primary productivity and biogeochemical cycles in the sea*, Environmental Book series, volume 43, pp. 213-237
- Chorus I & Bartram J (1999) *Toxic Cyanobacteria in Water: A Guide to Their Public Health Consequences, Monitoring and Management* London: E & FN Spon
- Chorus I, Welker M (2021) *Toxic cyanobacteria in water: a guide to their public health consequences, monitoring and management* p. 858. Taylor & Francis
- Coles J & Jones R (2000) Effect of temperature on photosynthesis-light response and growth of four phytoplankton species isolated from a tidal freshwater river. *Journal of Phycology* 36: 7-16
- Dick GJ, Duhaime MB, Evans JT, Errera RM, Godwin CM, Kharbush JJ, ... & Deneff VJ (2021) The genetic and ecophysiological diversity of *Microcystis*. *Environmental Microbiology* 23(12), 7278-7313
- Eiler A, Heinrich F & Bertilsson S (2011) Coherent dynamics and association networks among lake bacterioplankton taxa. *The ISME Journal* 6: 330-342
- Elliott J (2010) The seasonal sensitivity of Cyanobacteria and other phytoplankton to changes in flushing rate and water temperature. *Global Change Biology* 16: 864-876
- Elliott J, Jones I & Thackeray S (2006) Testing the Sensitivity of Phytoplankton Communities to Changes in Water Temperature and Nutrient Load, in a Temperate Lake. *Hydrobiologia* 559: 401-411
- Erdner D, Dyble J, Parsons M, Stevens R, Hubbard K, Wrabel M, Moore S, Lefebvre K, Anderson D, Bienfang P, Bidigare R, Parker M, Moeller P, Brand L & Trainer V (2008) Centers for Oceans and Human Health: a unified approach to the challenge of harmful algal blooms. *Environmental Health* 7: S2
- Esenkulova S, Sutherland B, Tabata A, Haigh N, Pearce C & Miller K (2020) Comparing metabarcoding and morphological approaches to identify phytoplankton taxa associated with harmful algal blooms. *FACETS* 5: 784-811
- Feist S & Lance R (2021) Genetic detection of freshwater harmful algal blooms: A review focused on the use of environmental DNA (eDNA) in *Microcystis aeruginosa* and *Prymnesium parvum*. *Harmful Algae* 110: 102124
- Fernald S, Caraco N & Cole J (2007) Changes in cyanobacterial dominance following the invasion of the zebra mussel *Dreissena polymorpha*: Long-term results from the Hudson River estuary. *Estuaries and Coasts* 30: 163-170
- Flombaum P, Gallegos L, Gordillo RA, Rincón J, Zabala LL, Jiao N, ... & Martiny C (2013) Present and future global distributions of the marine Cyanobacteria *Prochlorococcus* and *Synechococcus*. *Proceedings of the National Academy of Sciences* 110(24), 9824-9829
- Friedman M, Levin B (2005) Neurobehavioral effects of harmful algal bloom (HAB) toxins: A critical review. *Journal of the International Neuropsychological Society* 11: 331-338
- Fristachi A, Sinclair JL, Hall S, Berkman JA, Boyer G, Burkholder J, ... & Walker S (2008) Occurrence of cyanobacterial harmful algal blooms workgroup report. In *Cyanobacterial harmful algal blooms: state of the science and research needs* pp. 45-103. New York: Springer
- Gan N, Xiao Y, Zhu L, Wu Z, Liu J, Hu C & Song L (2012) The role of microcystins in maintaining colonies of bloom-forming *Microcystis* spp. *Environmental Microbiology* 14: 730-742

- Glibert PM, Burkholder JM (2006) The Complex Relationships Between Increasing Fertilization of the Earth, Coastal Eutrophication, and HAB Proliferation. In *The Ecology of Harmful Algae* pp 341-354. New York: Springer-Verlag
- Gobler C (2020) Climate Change and Harmful Algal Blooms: Insights and perspective. *Harmful Algae* 91: 101731
- Goodwin S, McPherson J & McCombie W (2016) Coming of age: ten years of next-generation sequencing technologies. *Nature Reviews Genetics* 17: 333-351
- Graham J & Jones J (2009) Microcystin in Missouri reservoirs. *Lake and Reservoir Management* 25: 253-263
- Hallegraeff G (1993) A review of harmful algal blooms and their apparent global increase. *Phycologia* 32: 79-99.
- Hallegraeff GM (2003) Harmful algal blooms: a global overview. In: *Manual on harmful marine microalgae* pp 33: 1-22
- Hampton S, Gray D, Izmet'eva L, Moore M & Ozersky T (2014) The Rise and Fall of Plankton: Long-Term Changes in the Vertical Distribution of Algae and Grazers in Lake Baikal, Siberia. *PLoS ONE* 9: e88920
- Hmelo L, Van Mooy B & Mincer T (2012) Characterization of bacterial epibionts on the cyanobacterium *Trichodesmium*. *Aquatic Microbial Ecology* 67: 1-14
- Huisman J, Codd G, Paerl H, Ibelings B, Verspagen J & Visser P (2018) Cyanobacterial blooms. *Nature Reviews Microbiology* 16: 471-483
- Huisman J, Hulot FD (2005) Population dynamics of harmful cyanobacteria. In *Harmful cyanobacteria* pp 143-176. Dordrecht: Springer
- Humbert J, Quiblier C & Gugger M (2010) Molecular approaches for monitoring potentially toxic marine and freshwater phytoplankton species. *Analytical and Bioanalytical Chemistry* 397: 1723-1732
- Jöhnk K, Huisman J, Sharples J, Sommeijer B, Visser P & Stroom J (2008) Summer heatwaves promote blooms of harmful cyanobacteria. *Global Change Biology* 14: 495-512
- Komárek J, Johansen JR (2015) Filamentous cyanobacteria. In *Freshwater Algae of North America* pp 135-235. Academic Press
- Kouzuma A & Watanabe K (2015) Exploring the potential of algae/bacteria interactions. *Current Opinion in Biotechnology* 33: 125-129
- Kromkamp J & Walsby A (1990) A computer model of buoyancy and vertical migration in cyanobacteria. *Journal of Plankton Research* 12: 161-183
- Lemes G, Kersanach R, da S. Pinto L, Dellagostin O, Yunes J & Matthiensen A (2008) Biodegradation of microcystins by aquatic *Burkholderia* sp. from a South Brazilian coastal lagoon. *Ecotoxicology and Environmental Safety* 69: 358-365
- Liboriussen L, Landkildehus F, Meerhoff M, Bramm M, Søndergaard M, Christoffersen K, Richardson K, Søndergaard M, Lauridsen T & Jeppesen E (2005) Global warming: Design of a flow-through shallow lake mesocosm climate experiment. *Limnology and Oceanography: Methods* 3: 1-9
- Marti C, Imberger J, Garibaldi L & Leoni B (2016) Using time scales to characterize phytoplankton assemblages in a deep subalpine lake during the thermal stratification period: Lake Iseo, Italy. *Water Resources Research* 52: 1762-1780

- Merel S, Walker D, Chicana R, Snyder S, Baurès E & Thomas O (2013) State of knowledge and concerns on cyanobacterial blooms and cyanotoxins. *Environment International* 59: 303-327
- Niu Y, Shen H, Chen J, Xie P, Yang X, Tao M, Ma Z & Qi M (2011) Phytoplankton community succession shaping bacterioplankton community composition in Lake Taihu, China. *Water Research* 45: 4169-4182
- O'Neil J, Davis T, Burford M & Gobler C (2012) The rise of harmful cyanobacteria blooms: The potential roles of eutrophication and climate change. *Harmful Algae* 14: 313-334
- Ozaki K, Ohta A, Iwata C, Horikawa A, Tsuji K, Ito E, Ikai Y & Harada K (2008) Lysis of cyanobacteria with volatile organic compounds. *Chemosphere* 71: 1531-1538
- Paerl H & Huisman J (2008) Blooms Like It Hot. *Science* 320: 57-58
- Paerl H & Huisman J (2009) Climate change: a catalyst for global expansion of harmful cyanobacterial blooms. *Environmental Microbiology Reports* 1: 27-37
- Paerl H & Otten T (2013) Harmful Cyanobacterial Blooms: Causes, Consequences, and Controls. *Microbial Ecology* 65: 995-1010
- Paerl H & Paul V (2012) Climate change: Links to global expansion of harmful cyanobacteria. *Water Research* 46: 1349-1363
- Paerl HW (1983) Partitioning of CO₂ fixation in the colonial cyanobacterium *Microcystis aeruginosa*: mechanism promoting formation of surface scums. *Applied and Environmental Microbiology* 46: 252-259
- Peeters F, Straile D, Loker A & Livingstone D (2007) Earlier onset of the spring phytoplankton bloom in lakes of the temperate zone in a warmer climate. *Global Change Biology* 13: 1898-1909
- Ploug H, Adam B, Musat N, Kalvelage T, Lavik G, Wolf-Gladrow D & Kuypers M (2011) Carbon, nitrogen and O₂ fluxes associated with the cyanobacterium *Nodularia spumigena* in the Baltic Sea. *The ISME Journal* 5: 1549-1558
- Pope PB, Patel BKC (2008) Metagenomic analysis of a freshwater toxic cyanobacteria bloom. *FEMS Microbiol Ecol* 64:9-27
- Rabalais N, Díaz R, Levin L, Turner R, Gilbert D & Zhang J (2010) Dynamics and distribution of natural and human-caused hypoxia. *Biogeosciences* 7: 585-619
- Rapala J, Sivonen K, Lyra C, Niemelä SI (1997) Variation of microcystins, cyanobacterial hepatotoxins, in *Anabaena* spp. as a function of growth stimuli. *Applied and environmental microbiology* 63(6), 2206-2212
- Robarts R & Zohary T (1987) Temperature effects on photosynthetic capacity, respiration, and growth rates of bloom-forming cyanobacteria. *New Zealand Journal of Marine and Freshwater Research* 21: 391-399
- Rowe MD, Anderson EJ, Wynne TT, Stumpf RP, Fanslow DL, Kijanka K, ... & Davis TW (2016) Vertical distribution of buoyant *Microcystis* blooms in a Lagrangian particle tracking model for short-term forecasts in Lake Erie. *Journal of Geophysical Research: Oceans* 121(7), 5296-5314
- Sanseverino, I., Pretto, P., António, D.C., Lahm, A., Facca, C., Loos, R., Skejo, H., Beghi, A., Pandolfi, F., Genoni, P. and Lettieri, T. (2022) Metagenomics analysis to investigate the microbial communities and their functional profile during cyanobacterial blooms in Lake Varese. *Microbial ecology*, 83: 850-868.
- Sarmiento J, Gruber N, Brzezinski M & Dunne J (2004) High-latitude controls of thermocline nutrients and low latitude biological productivity. *Nature* 427: 56-60
- Schirrmeister B, Gugger M & Donoghue P (2015) Cyanobacteria and the Great Oxidation Event: evidence from genes and fossils. *Paleoontology* 58: 769-785

- Schmittner A (2005) Decline of the marine ecosystem caused by a reduction in the Atlantic overturning circulation. *Nature* 434: 628-633
- Sellner K, Doucette G & Kirkpatrick G (2003) Harmful algal blooms: causes, impacts and detection. *Journal of Industrial Microbiology and Biotechnology* 30: 383-406
- Shen H, Niu Y, Xie P, Tao M & Yang X (2011) Morphological and physiological changes in *Microcystis aeruginosa* as a result of interactions with heterotrophic bacteria. *Freshwater Biology* 56: 1065-1080
- Sivonen K, Niemelä S., Niemi RM, Lepistö L, Luoma TH, Räsänen LA (1990) Toxic cyanobacteria (blue-green algae) in Finnish fresh and coastal waters. *Hydrobiologia* 190: 267-275
- Smayda TJ (1989) Primary production and the global epidemic of phytoplankton blooms in the sea: a linkage? In: *Novel phytoplankton blooms: causes and impacts of recurrent brown tide and other unusual blooms* pp 213-222. New York: Springer-Verlag
- Spungin D, Belkin N, Foster R, Stenegren M, Caputo A, Pujo-Pay M, Leblond N, Dupouy C, Bonnet S & Berman-Frank I (2018) Programmed cell death in diazotrophs and the fate of organic matter in the western tropical South Pacific Ocean during the OUTPACE cruise. *Biogeosciences* 15: 3893-3908
- Stauffer B, Bowers H, Buckley E, Davis T, Johengen T, Kudela R, McManus M, Purcell H, Smith G, Vander Woude A & Tamburri M (2019) Considerations in Harmful Algal Bloom Research and Monitoring: Perspectives From a Consensus-Building Workshop and Technology Testing. *Frontiers in Marine Science* 6:399
- Takamura N, Iwakuma T, Yasuno M (1985) Photosynthesis and primary production of *Microcystis aeruginosa* Kütz. in Lake Kasumigaura. *Journal of Plankton Research* 7: 303-312
- Thomas M & Litchman E (2016) Effects of temperature and nitrogen availability on the growth of invasive and native cyanobacteria. *Hydrobiologia* 763: 357-369
- Valentini A, Taberlet P, Miaud C, Civade R, Herder J, Thomsen PF, ... & Dejean T (2016) Next-generation monitoring of aquatic biodiversity using environmental DNA metabarcoding. *Molecular Ecology* 25(4), 929-942
- Van Hannen E, Zwart G, van Agterveld M, Gons H, Ebert J & Laanbroek H (1999) Changes in Bacterial and Eukaryotic Community Structure after Mass Lysis of Filamentous Cyanobacteria Associated with Viruses. *Applied and Environmental Microbiology* 65: 795-801
- Verspagen J, Van de Waal D, Finke J, Visser P, Van Donk E & Huisman J (2014) Rising CO₂ Levels Will Intensify Phytoplankton Blooms in Eutrophic and Hypertrophic Lakes. *PLoS ONE* 9: e104325
- Visser P, Verspagen J, Sandrini G, Stal L, Matthijs H, Davis T, Paerl H & Huisman J (2016) How rising CO₂ and global warming may stimulate harmful cyanobacterial blooms. *Harmful Algae* 54: 145-159
- Visser PM, Ibelings BW, Mur LR (1995) Autumnal sedimentation of *Microcystis* spp. as result of an increase in carbohydrate ballast at reduced temperature. *Journal of Plankton Research* 17: 919-933
- Wagner C & Adrian R (2009) Cyanobacteria dominance: Quantifying the effects of climate change. *Limnology and Oceanography* 54: 2460-2468
- Walsby AE (1981) Cyanobacteria: planktonic gas-vacuolate forms. In: *The prokaryotes* pp 224-235. Berlin: Springer
- Walsby AE, Schanz F (2002) Light-dependent growth rate determines changes in the population of *Planktothrix rubescens* over the annual cycle in Lake Zürich, Switzerland. *New Phytologist* 154: 671-687

Whitton BA, Potts M (2012) Introduction to the cyanobacteria. In *Ecology of Cyanobacteria II* pp. 1-13. Dordrecht: Springer

Winder M, Sommer U (2012) Phytoplankton response to a changing climate. *Hydrobiologia* 698: 5-16.

Worden AZ, Follows MJ, Giovannoni SJ, Wilken S, Zimmerman AE, Keeling PJ (2015) Rethinking the marine carbon cycle: factoring in the multifarious lifestyles of microbes. *Science* 347:1257594.

Xiao M, Li M, Reynolds CS (2018) Colony formation in the cyanobacterium *Microcystis*. *Biological Reviews* 93:1399-1420

Xie, M., Ren, M., Yang, C., Yi, H., Li, Z., Li, T. and Zhao, J., (2016). Metagenomic analysis reveals symbiotic relationship among bacteria in *Microcystis*-dominated community. *Frontiers in Microbiology*, 7: 56.

Zheng G, Xu R, Chang X, Hilt S & Wu C (2013) Cyanobacteria can allelopathically inhibit submerged macrophytes: Effects of *Microcystis aeruginosa* extracts and exudates on *Potamogeton malaianus*. *Aquatic Botany* 109: 1-7

8. APPENDICES

Table S1. Mesocosm sampling data.

Week	Date	Condition	Number of samples
1	08.07.21	Stratified	24
2	15.07.21	Stratified	24
3	22.07.21	Mixed	24
4	29.07.21	Mixed	24
5	05.08.21	Stratified	24
6	12.08.21	Stratified	24
7	19.08.21	Mixed	24
8	26.08.21	Mixed	24

Table S2. Primers for identification of *Microcystis sp.*-specific functional genes.

Target gene	Sequence name	Sequence (5' to 3')
<i>mcyE</i>	mcyE-F2	GAAATTTGTGTAGAAGGTGC
	MicmcyE-R8	CAATGGGAGCATAACGAG
<i>capD</i>	MAE12350-For	TCTATGGTGCGGGGATTGTGGGT
	MAE12350-Rev	GGGGAGGGACGGTTTTGATGACG
<i>csaB</i>	MAE08580-For	AAACAACGACAATCTTCTGCTGC
	MAE08580-Rev	CAATTTACGTCCCCATCCCCTAT
<i>tagH</i>	MAE42490-For	CCGACAAAGGGACAGGTGAGA
	MAE42490-Rev	CGCAAATCCTAAACGAGCCAC
<i>epsL</i>	MAE49260-For	CGATGGGTGCGTTATCTTCC
	MAE49260-Rev	GCCGATTACTGGCTGTCCTG
<i>rfbB</i>	MAE42470-For	AGTGGCGGGGTATGATGTGAA
	MAE42470-Rev	TCTGGGGATTGGGGATATGGT
<i>cpsF</i>	MAE41480-For	TAGCAGCCCAAGTTCTTCTCAA
	MAE41480-Rev	TTCAACCCGTGTAAAAGACTCAA
<i>gvpC</i>	gvpC-f	TCTCTAGCCGTTTCGCTTCA
	gvpC-r	TGGAAAAGTTCCGCCAGGAG
<i>gvpA</i>	gvpA1A2A3-f	CCCTACAGGGTTTTGCAGAT
	gvpA1A2A3-r	TTCCTACCAAAGAGACGCG

Table S3. Demultiplexing results of 8 sequencing runs.

Week	1	2	3	4	5	6	7	8
Number of reads	5,559,659	5,302,319	6,829,112	5,372,895	6,412,082	3,942,752	3,445,993	3,372,685

Adapters detected	96.80%	96.83%	95.36%	95.92%	95.11%	93.46%	94.06%	96.19%
A1-T	1.44%	12.27%	4.50%	2.19%	3.69%	0.86%	4.99%	5.76%
A1-B	6.72%	2.37%	3.98%	3.12%	3.82%	0.77%	1.28%	4.62%
A2-T	8.16%	10.21%	5.60%	11.79%	5.50%	2.18%	6.15%	7.35%
A2-B	11.84%	6.89%	5.31%	13.53%	5.15%	5.17%	2.32%	8.55%
A3-T	0.22%	1.92%	2.19%	1.43%	3.93%	4.08%	1.21%	2.01%
A3-B	12.45%	8.14%	2.41%	3.13%	4.44%	6.17%	5.85%	8.09%
D1-T	0.56%	1.86%	2.12%	0.76%	3.67%	1.26%	2.12%	0.08%
D1-B	1.98%	4.34%	2.02%	1.21%	1.91%	1.00%	0.13%	0.12%
D2-T	5.87%	2.05%	5.43%	4.35%	4.95%	0.11%	2.57%	6.57%
D2-B	1.58%	2.13%	5.20%	1.08%	4.58%	1.36%	4.59%	0.96%
D3-T	1.33%	3.71%	5.44%	3.56%	4.74%	5.17%	0.89%	9.51%
D3-B	13.85%	8.03%	5.81%	21.21%	4.32%	5.58%	7.27%	5.17%
F1-T	5.24%	2.13%	4.94%	3.31%	3.37%	6.78%	4.66%	1.98%
F1-B	6.33%	8.73%	5.21%	2.97%	3.60%	7.25%	4.70%	5.17%
F2-T	0.96%	3.04%	3.95%	3.32%	2.17%	6.26%	2.83%	3.38%
F2-B	2.75%	2.56%	3.61%	2.42%	5.19%	0.06%	4.59%	2.52%
F3-T	2.06%	2.04%	4.81%	1.35%	3.92%	0.24%	1.45%	1.05%
F3-B	1.31%	0.97%	4.84%	2.01%	3.70%	1.45%	6.68%	2.26%
G1-T	1.47%	2.51%	2.14%	0.96%	3.75%	8.67%	4.91%	5.58%
G1-B	2.58%	0.49%	2.95%	1.03%	3.97%	4.32%	5.59%	1.20%
G2-T	2.26%	0.97%	3.64%	1.97%	2.23%	5.40%	6.38%	3.56%
G2-B	1.77%	0.49%	1.15%	1.35%	1.99%	4.24%	2.47%	2.21%
G3-T	1.13%	1.34%	4.37%	1.80%	3.04%	7.62%	5.22%	6.35%
G3-B	2.95%	7.64%	3.71%	6.07%	7.46%	7.46%	5.23%	2.16%
None	2.48%	2.43%	3.99%	3.32%	4.19%	5.64%	4.96%	3.09%

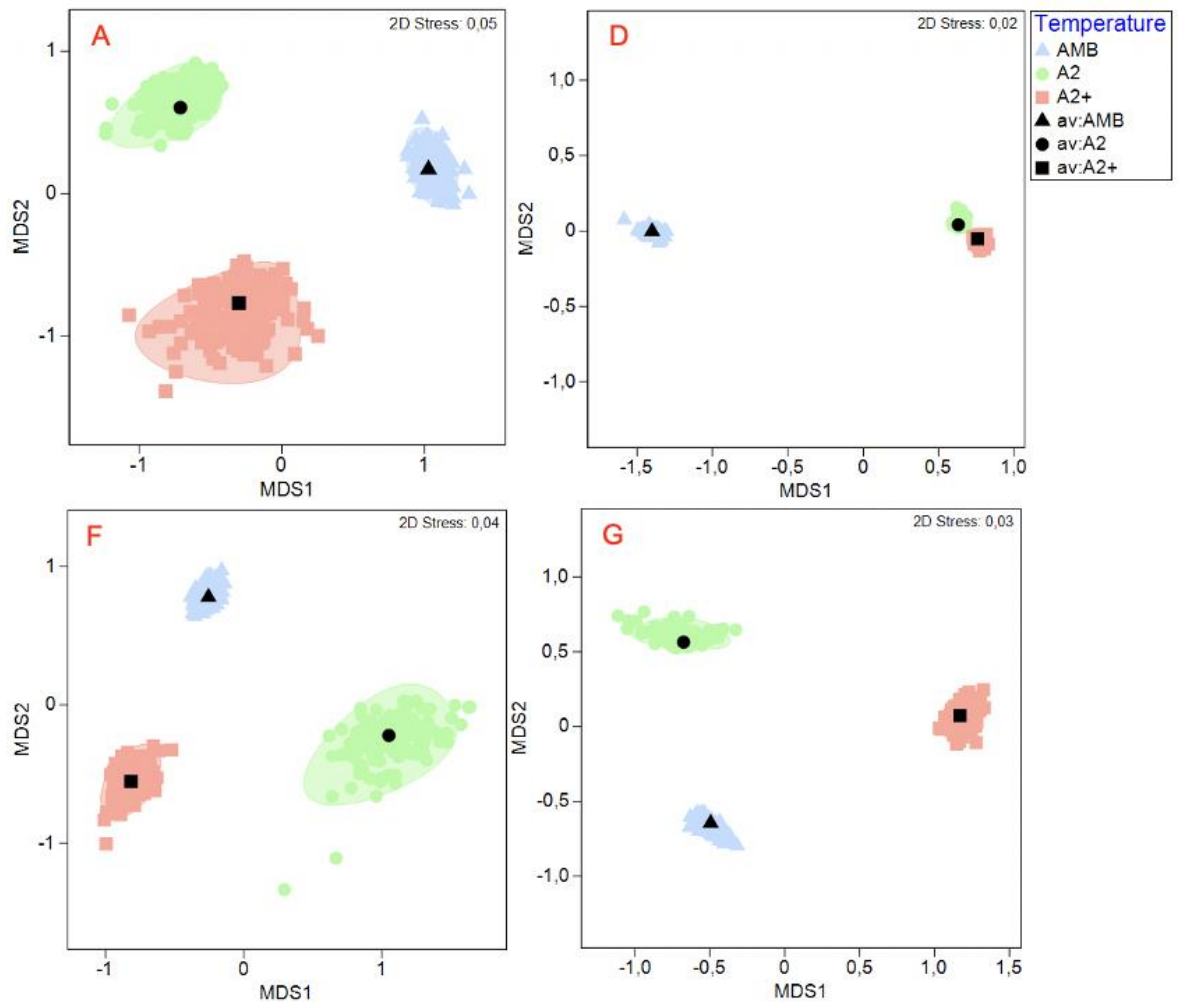


Figure S1. Bootstrap regions for community composition averages in all tanks across varying temperature regimes (AMB – ambient, A2 – IPCC A2, A2+ – IPCC A2+) in an nMDS space with 150 bootstraps per group and 95% coverage.

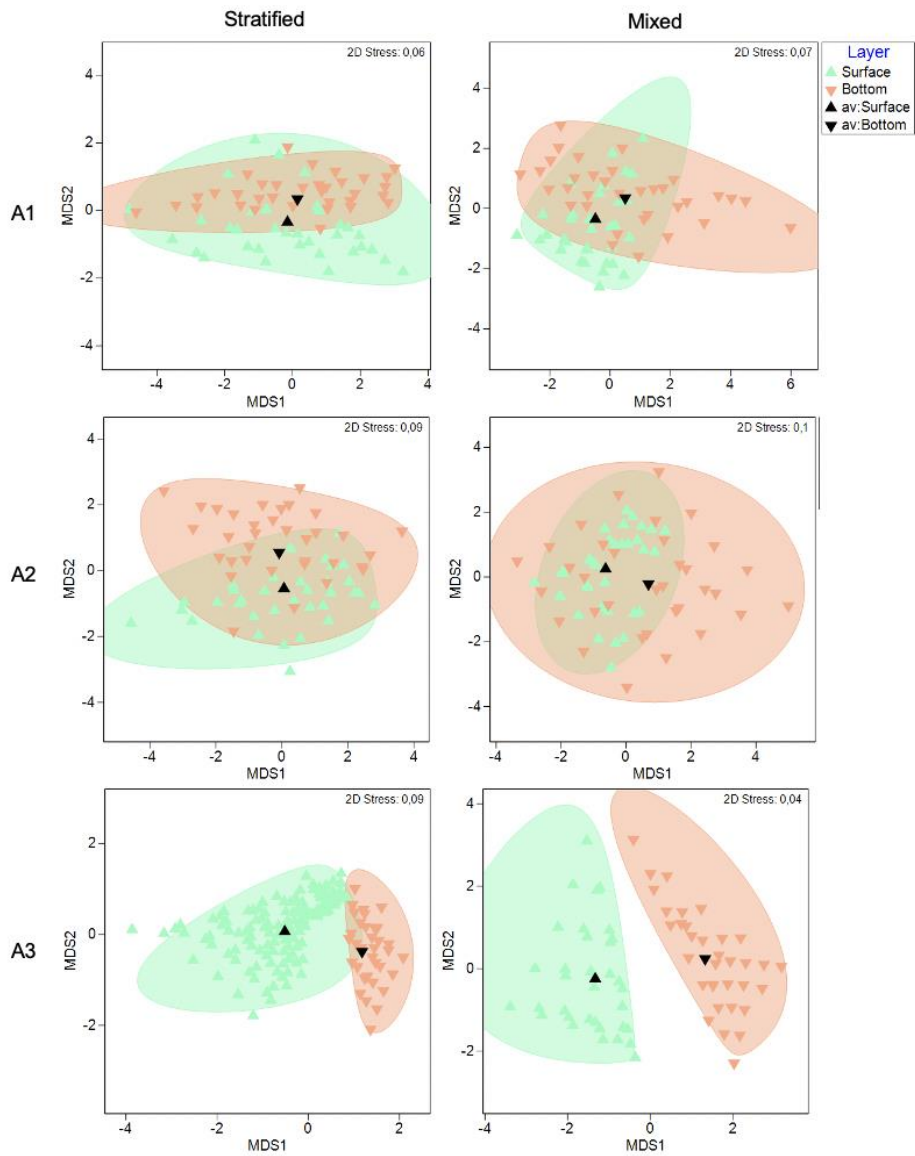


Figure S2. Bootstrap regions for community composition averages in tanks A across varying temperature regimes (A1 – ambient, A2 – IPCC A2, A3- IPCC A2+) during stratified and mixed periods in an nMDS space with 150 bootstraps per group and 95% coverage.

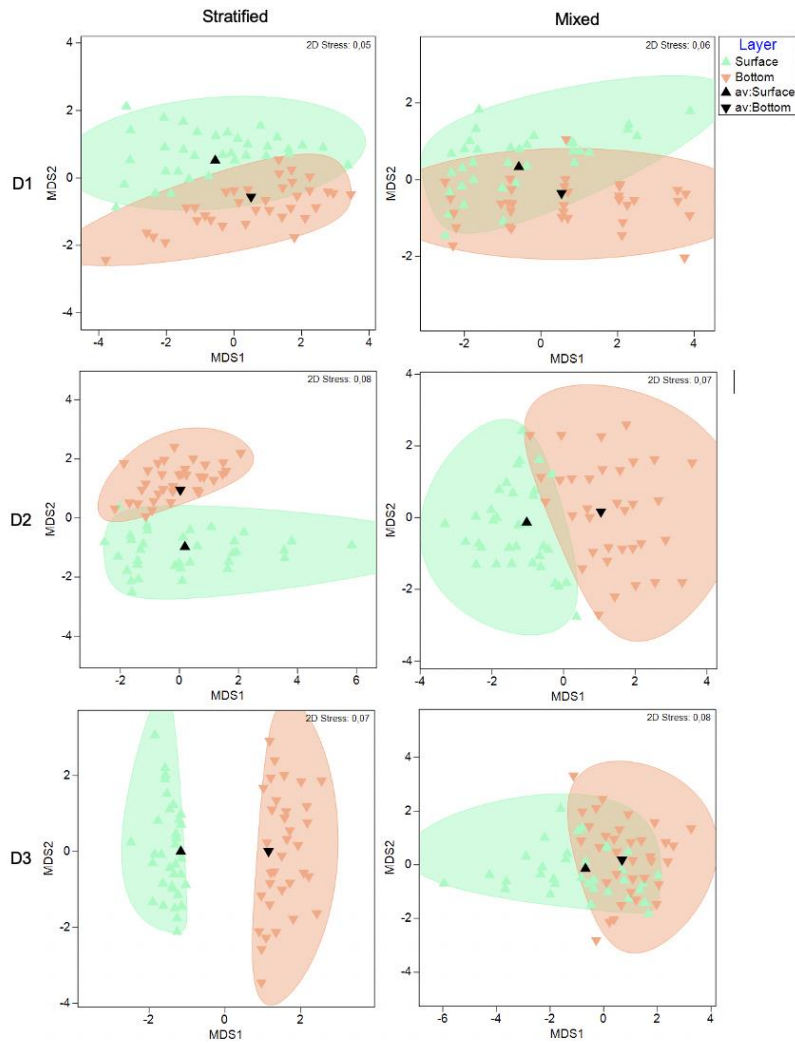


Figure S3. Bootstrap regions for community composition averages in tanks D across varying temperature regimes (D1 – ambient, D2 – IPCC A2, D3- IPCC A2+) during stratified and mixed periods in an nMDS space with 150 bootstraps per group and 95% coverage.

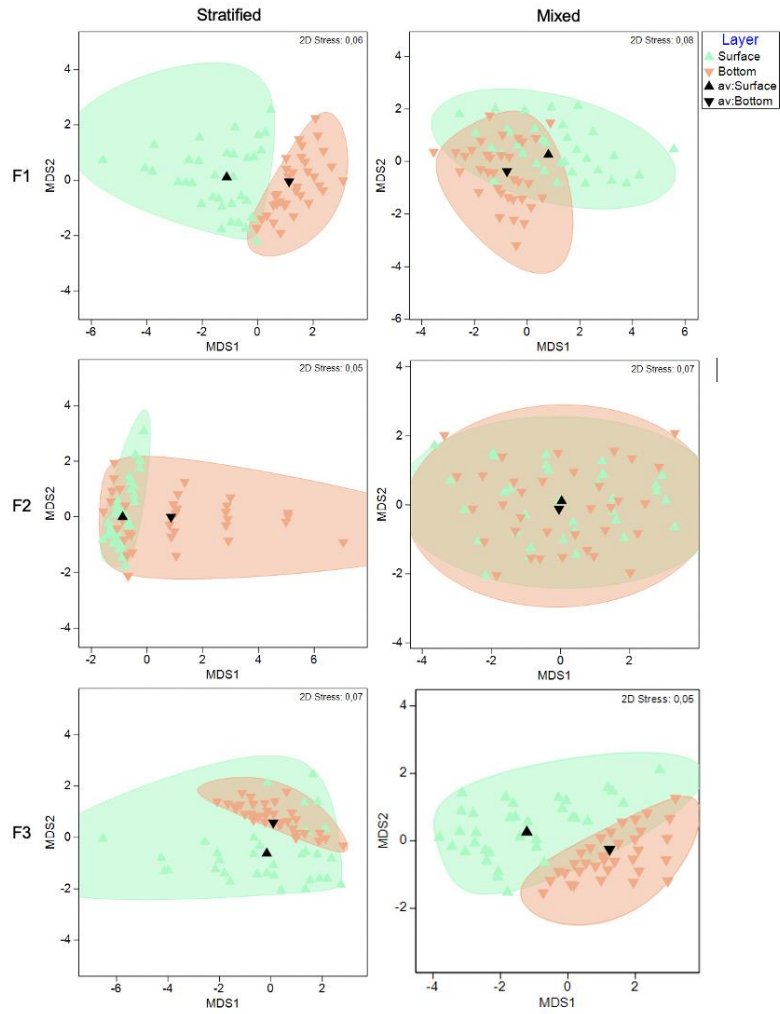


Figure S4. Bootstrap regions for community composition averages in tanks F across varying temperature regimes (F1 – ambient, F2 – IPCC A2, F3- IPCC A2+) during stratified and mixed periods in an nMDS space with 150 bootstraps per group and 95% coverage.

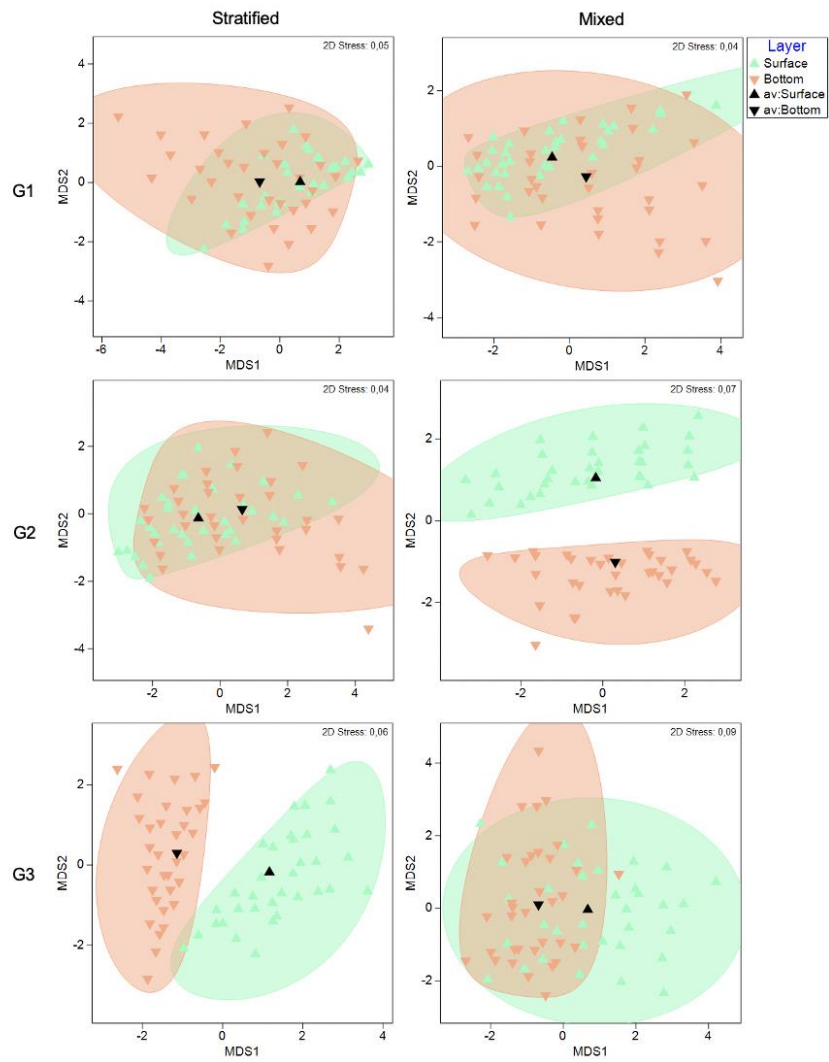


Figure S5. Bootstrap regions for community composition averages in tanks G across varying temperature regimes (G1 – ambient, G2 – IPCC A2, G3- IPCC A2+) during stratified and mixed periods in an nMDS space with 150 bootstraps per group and 95% coverage.

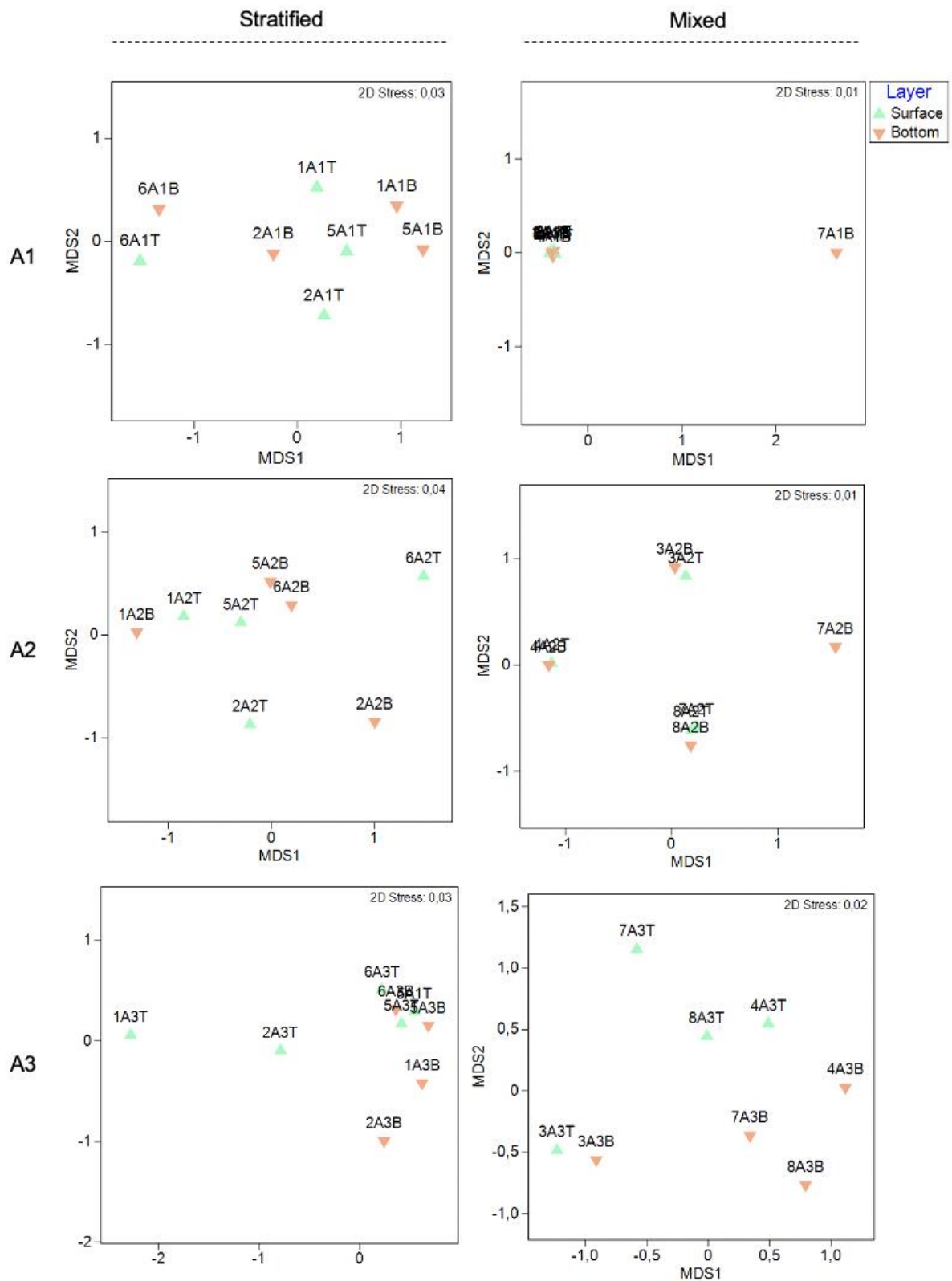


Figure S6. Multidimensional scaling of Bray–Curtis distance matrix of community compositions during the course of the experiment. NMDS ordination plots indicate clustering across varying sampling depths: surface and bottom (AMB - ambient temperature, A2 – IPCC A2, A2+ - IPCC A2+ temperature regime) in tanks A.

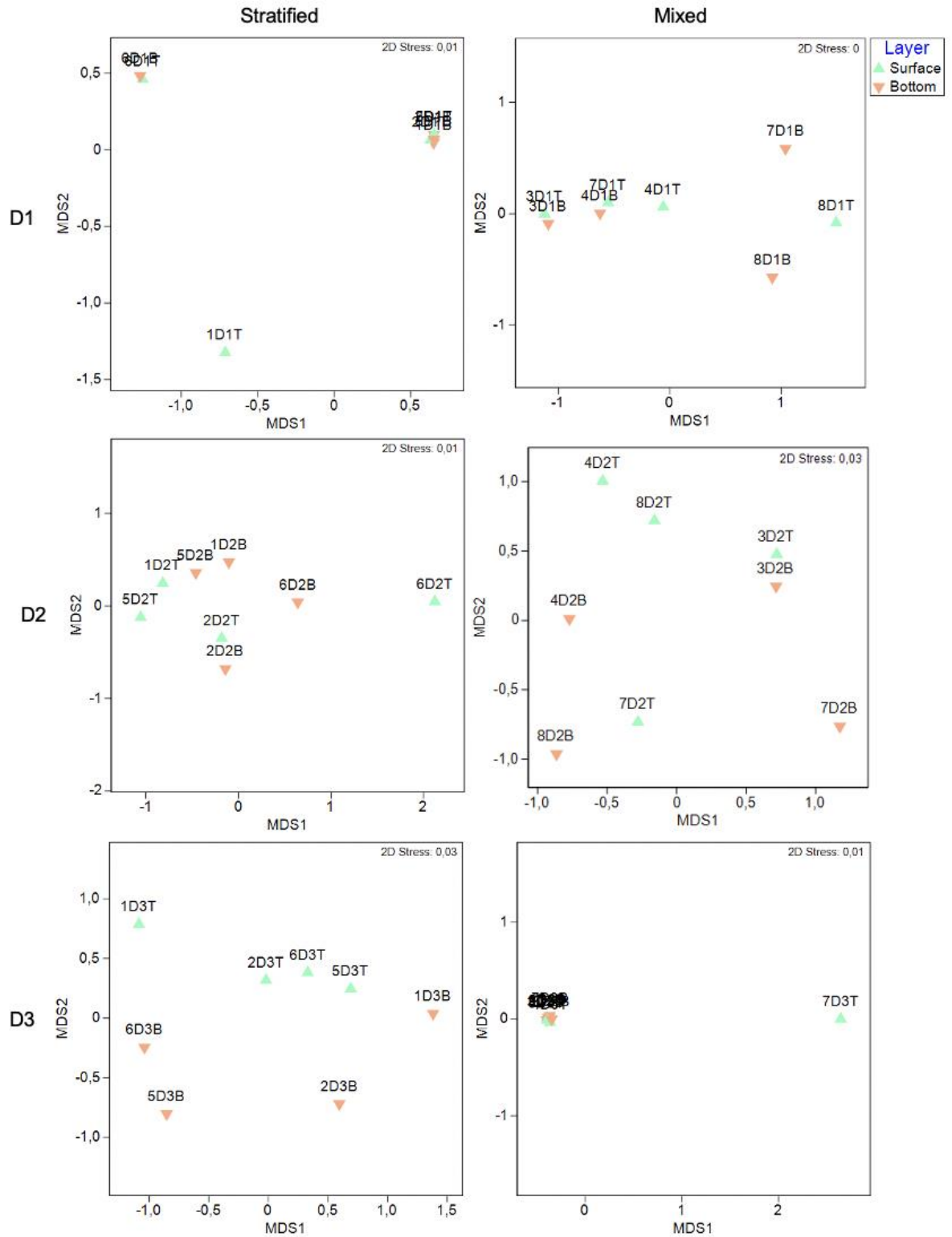


Figure S7. Multidimensional scaling of Bray–Curtis distance matrix of community compositions during the course of the experiment. NMDS ordination plots indicate clustering across varying sampling depths: surface and bottom (AMB - ambient temperature, A2 – IPCC A2, A2+ - IPCC A2+ temperature regime) in tanks D.

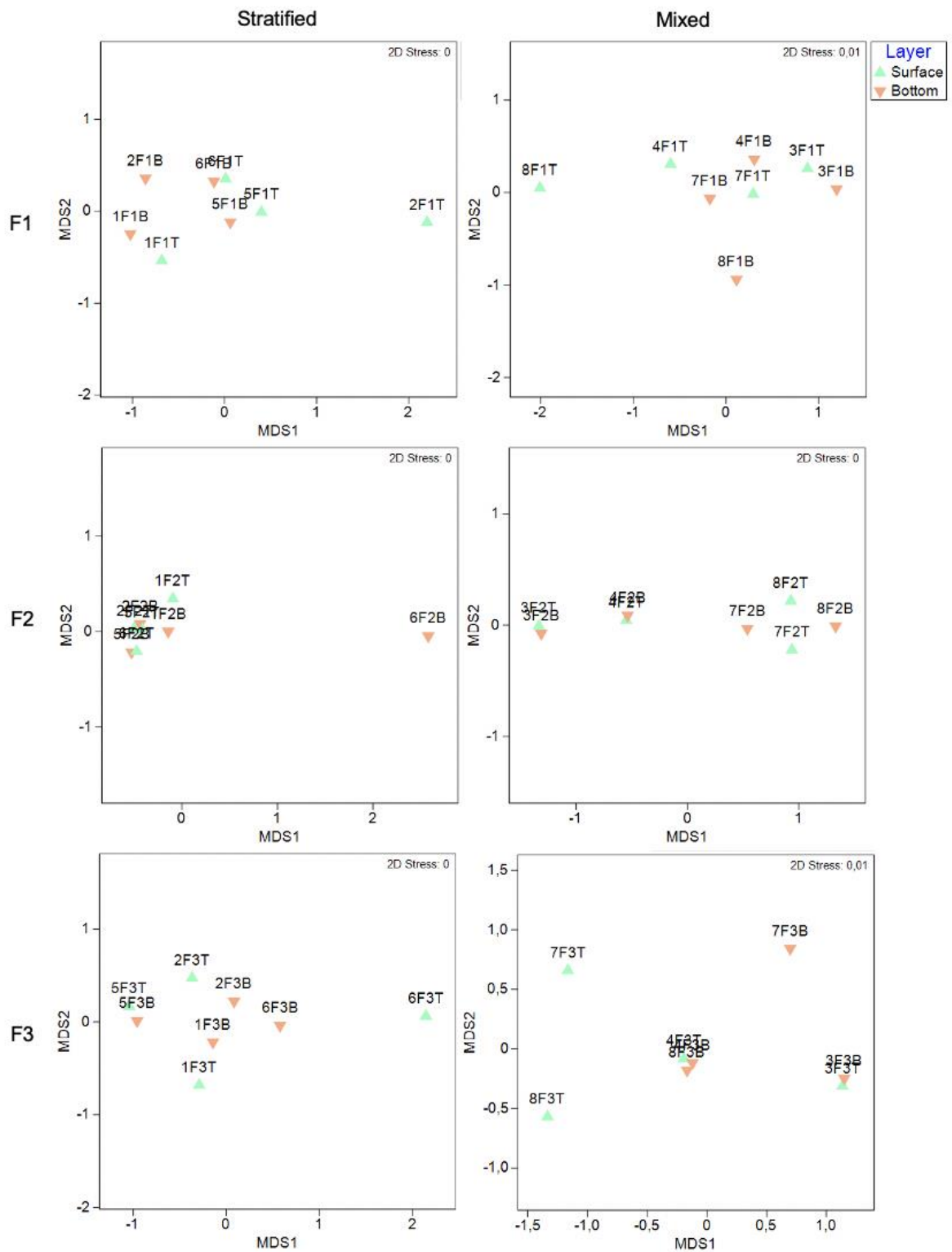


Figure S8. Multidimensional scaling of Bray–Curtis distance matrix of community compositions during the course of the experiment. NMDS ordination plots indicate clustering across varying sampling depths: surface and bottom (AMB - ambient temperature, A2 – IPCC A2, A2+ - IPCC A2+ temperature regime) in tanks F.

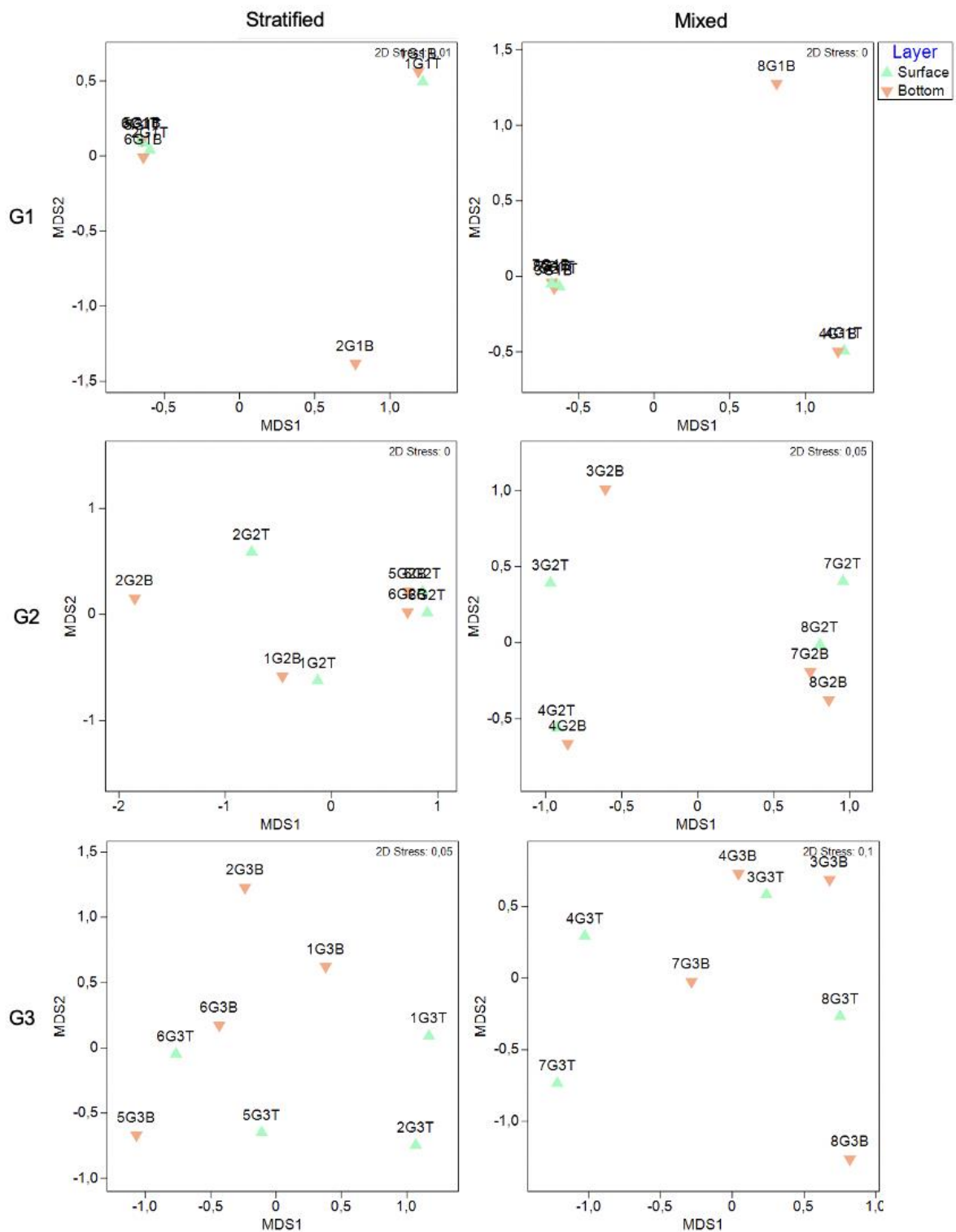


Figure S9. Multidimensional scaling of Bray–Curtis distance matrix of community compositions during the course of the experiment. NMDS ordination plots indicate clustering across varying sampling depths: surface and bottom (AMB - ambient temperature, A2 – IPCC A2, A2+ - IPCC A2+ temperature regime) in tanks G.